

POLITECNICO DI TORINO

Corso di Laurea in Ingegneria Meccanica



MASTER DEGREE THESIS

Development of the test bench of an EMA for prognostic: ideation and realization in additive manufacturing of the conceptual prototype for a reduction gear

Academic tutors

Prof. Paolo Maggiore

Ing. Matteo Davide Lorenzo Dalla Vedova

Student

Guido Riva

April 2019

Table of contents

List of Figures	III
List of Tables.....	VII
Credits	1
Introduction	3
1. Flight Controls	5
1.1. Primary and secondary flight controls	9
2. Actuation Systems	11
2.1. Hydromechanical Actuation Systems	13
2.2. Electrohydraulic Actuation Systems	14
2.3. Electrohydrostatic Actuation Systems (EHA).....	17
2.4. Electromechanical Actuation Systems (EMA).....	18
3. Fused Deposition Modeling	19
3.1. Technology.....	19
3.2. Materials.....	22
3.2.1. ABS (Acrylonitrile Butadiene Styrene)	22
3.2.2. PLA (Polylactic Acid).....	23
3.2.3. PVA (Polyvinyl Alcohol)	25
3.2.4. Other materials	26
3.3. Machine.....	27
3.3.1. Software Ultimaker Cura	29
3.3.2. FABUI application.....	37
4. Production of the functional prototype of the reduction gear.....	39
4.1. CAD design and production conditions for FDM.....	39
4.2. Reduction ratio.....	42
4.3. Analysis of the first gear wheel.....	45
4.4. Meshing between two gear wheels.....	49
4.5. Assembly of the first planetary gear	53

4.6.	Assembly of the solar gear	56
4.7.	Design of the internal gears	60
4.7.1.	Design of the lateral internal gears	61
4.7.2.	Design of the central internal gear	64
4.8.	Assembly of the reduction gear	68
4.9.	Coupling between the reduction gear and the encoder	71
4.9.1.	Encoder utilized	72
4.9.2.	Support for the encoder	73
4.9.3.	Spur gear wheel	75
5.	Future developments and conclusions	77
5.1.	Future developments	77
5.2.	Conclusions	80
	Bibliography	81

List of Figures

Figure 1 Graphical representation of the hinge moment	5
Figure 2 Conceptual scheme of enhanced flight controls.....	7
Figure 3 Control surfaces of an airliner	9
Figure 4 Control scheme of an actuation system.....	11
Figure 5 Rotary actuators with screw-nut system and with ball screw system	12
Figure 6 Diagram of a conventional hydromechanical servomechanism.....	13
Figure 7 Diagram of a hydromechanical servomechanism with electric autopilot.....	13
Figure 8 Diagram of an electrohydraulic servomechanism.....	14
Figure 9 Flapper nozzle valve	14
Figure 10 Jet pipe valve.....	15
Figure 11 DDV valve	15
Figure 12 Scheme of an EHA.....	17
Figure 13 Scheme of an EMA system	18
Figure 14 System for the fusion and deposition of the material for FDM	19
Figure 15 Movements in a machine for FDM	20
Figure 16 FabTotum Core Pro 2018 machine	28
Figure 17 Example of a view of one of the produced components, once loaded into the Cura software	29
Figure 18 Settings used to manage the quality of the elements that make up the pieces produced	30
Figure 19 Settings used to manage the thickness of external layers	31
Figure 20 Infill settings for the pieces produced	31
Figure 21 Settings for temperature and extrusion speed	32
Figure 22 Distance and speed values of retraction of the material.....	34
Figure 23 Cooling fan management parameters.....	34
Figure 24 Assigned values for the generation of support areas.....	35

Figure 25 Example of preview of the component divided into layers	36
Figure 26 FABUI interface during the printing process	37
Figure 27 Controls provided by the FABUI application	38
Figure 28 Section of the reduction gear to be produced for Additive Manufacturing.....	39
Figure 29 CAD model of gear wheels: gear wheel 21l (a) and gear wheel 21r (b), with specular toothing angles, and gear wheel 20 (c), double-helical	40
Figure 30 Diagram of the structure of the reduction gear.....	42
Figure 31 First printing of a gear wheel, without the manufacturing fixes for FDM, and detail of the support structures in the grooves	45
Figure 32 Gear wheel produced without grooves and internal supports	46
Figure 33 Structure of the gear wheel divided into three components	47
Figure 34 Detail of the cylinders used for the coupling of the flanges with the gear wheel	47
Figure 35 Contact between adjacent flanges in the final assembly	49
Figure 36 Gear wheels used in the first meshing test	50
Figure 37 Second meshing test, to have contact between adjacent flanges.....	50
Figure 38 Final result of the meshing test, with contact of the adjacent flanges.....	51
Figure 39 Detail of the meshing between adjacent gear wheels.....	51
Figure 40 Final measurements of double-angle gear wheels.....	52
Figure 41 Assembly of the planetary gear, obtained from the CAD of the reduction gear	53
Figure 42 Assembly composed of a flange and a steel ring	53
Figure 43 Flange and spacer used.....	54
Figure 44 Final assembly of the planetary gear	55
Figure 45 Drawing made with the CAD software, showing the final structure that planetary gear must have	56
Figure 46 Test toothing that reproduces the internal gear	57
Figure 47 Section view of the adapter, to highlight the area that houses the nut	58
Figure 48 Final design of the adapter	58

Figure 49 Coupling of a bearing with the PLA outer ring	59
Figure 50 Final assembly of the rotating solar A	59
Figure 51 CAD design of the internal gears of the reduction gear.....	60
Figure 52 CAD design of one of the two lateral internal gears.....	61
Figure 53 First printing result of the lateral internal gear	62
Figure 54 Detail of the teeth profile obtained with the first attempt	62
Figure 55 Profile of the teeth obtained in the second attempt, following the narrowing of the profile	63
Figure 56 Final structure of the side crown, coupled with the steel ring	63
Figure 57 Central internal gear of the reduction gear.....	64
Figure 58 Detail of one of the two side elements with the corresponding slot, after the redesign.....	65
Figure 59 Final result of the coupling between the outer component and the side elements	66
Figure 60 Detail of the coupling between the outer part and the inner part with the double-helical toothing	66
Figure 61 Exploded view of the central internal gear, after redesign operations.....	67
Figure 62 Reduction gear assembled.....	70
Figure 63 CAD drawing of the coupling between the support for the encoder and the spur gear wheel.....	71
Figure 64 CAD drawing of the encoder support	73
Figure 65 Support for the encoder	74
Figure 66 CAD drawing of the coupling wheel between the encoder and the rotating solar B	75
Figure 67 Coupling gear wheel between the encoder and the rotating solar B.....	76

List of Tables

Table 1 Mechanical properties of the different types of ABS offered by Stratasys	22
Table 2 Mechanical properties of the PLA, obtained from the Stratasys datasheets	23
Table 3 Characteristics of the encoder used for rotation detection	72
Table 4 Example of variation of gear wheel radii in the event of changes to the modulus and the number of teeth	78

Credits

Non sono mai stato molto bravo a scrivere dediche e mettere nero su bianco i miei pensieri, ma ritengo che al termine di un percorso come quello che ha portato alla mia laurea magistrale sia corretto (oltre che molto soddisfacente, lo ammetto!) rivolgere un pensiero a tutti coloro che hanno dedicato in questi cinque anni anche solo qualche attimo del loro tempo per darmi conforto e una spinta ad andare avanti, quando necessario.

Innanzitutto, vorrei ringraziare il professor Paolo Maggiore e l'ingegner Matteo Dalla Vedova per avermi indirizzato a questo lavoro di tesi e per avermi dedicato il loro tempo, trovando anche per me uno spazio nel loro ufficio sempre affollatissimo. Ho avuto l'occasione di lavorare con due delle menti più brillanti che abbia conosciuto, oltre che con due persone capaci di dare conforto a me e alla mia famiglia anche nei momenti di difficoltà. Non basteranno mai le parole per descrivere quanto sia grato di aver potuto lavorare in questo clima di serenità e allegria.

Sempre in tema di menti brillanti, un ringraziamento speciale va anche all'ingegner Pier Carlo Berri, colui che è stato il vero e proprio ideatore del lavoro su cui si basa questa mia tesi magistrale. Grazie per avermi accolto nell'ufficio dei dottorandi e aver sopportato la mia invadenza, e grazie per avermi dedicato così tanto tempo per poter vedere la nascita di quella che, in questi mesi, è diventata un po' la nostra creatura (con le gioie e i fallimenti che questo ha comportato). Ho sempre ascoltato i tuoi consigli e cercato di assorbire più nozioni possibili e sono sicuro che quanto appreso potrà essere un ottimo punto di partenza per poter delineare quella che sarà la mia figura professionale.

Non sarei potuto arrivare a questo traguardo senza l'appoggio dei miei amici. Avete sopportato i miei "no" molte delle volte in cui mi proponevate di uscire, avete festeggiato con me per i miei successi e mi avete consolato quando lo sconforto prendeva il sopravvento. Grazie, perché non è facile aiutare una persona, specie quando questa è testarda e orgogliosa come sono io.

Sono orgoglioso di poter ringraziare così tante persone, ma c'è qualcosa di cui vado ancora più orgoglioso: la mia famiglia.

Prima di tutto, vorrei ringraziare il supporto datomi dalle nonne (nonna Carla e nonna Marisa). Le parole dolci, le cene a Natale e a Pasqua tutti insieme e le preghiere per i miei esami sono solo alcuni dei motivi per i quali il vostro appoggio è stato fondamentale.

Vorrei anche dedicare qualche parola ai miei due ingegneri preferiti: papà Paolo e Giorgio, mio fratello. Siamo tutti e tre testardi e, tra poco, tutti e tre ingegneri. Siete stati la mia ispirazione in questi anni, per la vostra dedizione al lavoro e per la vostra intelligenza. Se ho imparato a dedicarmi ai miei progetti senza sosta e con passione è grazie a voi.

La persona che mi ha dedicato tutto il suo tempo, le sue energie e la sua pazienza (e quanta pazienza!) è mia mamma, Anna. Sei la donna più forte che conosca, perché sei stata capace di donarmi il tuo amore incondizionato, sopportando le litigate e le alzate di ingegno che ogni tanto mi contraddistinguono (e sopportando la presenza di tre ingegneri, o quasi tali, in casa)... ma non hai mai mollato e hai sempre creduto che questa impresa, la laurea del tuo figlio piccolo, fosse realizzabile. Insieme abbiamo studiato, pianto e riso quando era il momento. Abbiamo combattuto due battaglie in quest'ultimo anno e con questo lavoro di tesi possiamo dire che le abbiamo vinte entrambe.

Non sono mai stato molto bravo a scrivere dediche e mettere nero su bianco i miei pensieri, ma con queste poche righe voglio soltanto dirvi una cosa: GRAZIE!

Torino, 11 aprile 2019

Introduction

This thesis consists in the study and application of the steps which are necessary for the production of a reduction gear, used as part of the test bench of an electromechanical actuation system (EMA).

The function of the reducer is to adjust the high input speed, coming from the shaft of an electric motor, to a lower speed value, thus allowing the movement of a screw-nut or ball screw system. The discussion will therefore require the introduction of the systems used for the implementation of flight controls and an explanation of the operating principle of an EMA, in order to understand the real functionality of the designed component.

The work also has the purpose of describing the process of making the reducer itself, analyzing the errors and corrections that led to obtaining the final result, in such a way as to outline a univocal and rapid procedure, which allows to replicate the component obtained, in case it will be necessary.

The main objective of the thesis is to obtain a conceptual prototype, which is a model that takes into account purely the geometry and not the material, nor the production technique that should be used to obtain the reduction gear, in case it would work in situations of realistic loads (for example, in the case of loads close to those for the regulation of a real EMA). The reduction gear itself must be tested, in fact, in reduced load conditions and can be used for educational purposes.

The discussion also aims to define the dependence of the properties of the final component on the methodology used. The properties obtained depend mainly on the additive manufacturing technique used, namely Fused Deposition Modeling (FDM), useful for prototyping works with desktop printers. The iterative procedure used allows to obtain the dependence of the properties of the components on the parameters entered in the machine. To complete the study, therefore, the fundamental parameters for the management of the printing operations of the components that make up the reduction gear have been listed and analyzed..

For the production of the prototype, PLA was used; it is a material with low mechanical strength, but sufficient for the intended purpose, which is that of obtaining the semi-definitive geometry of the component. The component itself must be tested, at the end of the production, without load (the gear, therefore, will be made to run unloaded); consequently, the mechanical stresses will be reduced compared to those that a reduction gear of the type described in the following pages should hold up during the actual work phase.

1. Flight Controls

The purpose of flight controls is to change the shape of aerodynamic surfaces, to generate forces and moments that could change the attitude and trajectory of an aircraft. Given an airfoil with a movable surface (Figure 1), immersed in an air flow at the speed V_∞ , when the airfoil itself varies its attitude (α), the movable surface tends to get aligned to the direction of the flow, tilting of an angle δ , called “deflection angle”. In order to maintain a neutral position of the moving surface, it will be necessary to apply a suitable hinge moment. By applying muscle strength, the pilot will generate this moment by acting on the commands connected to the flight controls.

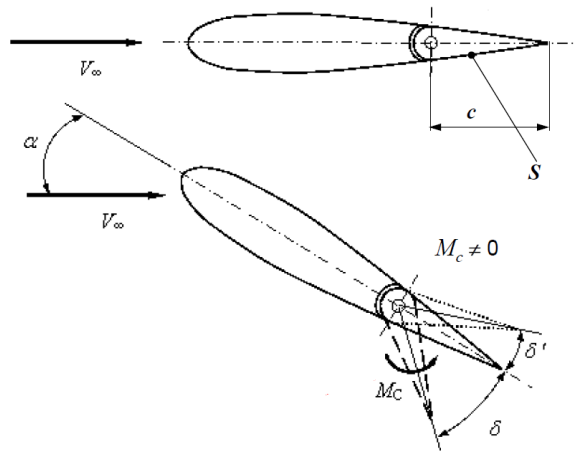


Figure 1 Graphical representation of the hinge moment

Mathematically we will have:

$$M_C = C_{M_C} \frac{1}{2} \rho V_\infty^2 S c$$

Where C_{M_C} represents the coefficient of the hinge moment, written as:

$$C_{M_C} = k_0 + k_\alpha \alpha + k_\delta \delta$$

In which the three addends are, respectively, linked to the form factor of the complete profile, to the incidence of the complete profile and to the deflection angle of the moving surface.

The flight controls are divided into two large families: primary and secondary. The big difference between primary and secondary flight controls consists in the fact that the primary controls are used continuously in all phases of the flight, while the secondary ones are used in some special cases (for example take-off or landing) or for some maneuvers.

Flight controls may be reversible or enhanced.

The reversible controls are purely mechanical and are driven by the strength of the human being, possibly assisted by aerodynamic devices. This is the case of aerodynamically compensated controls, with appendices that extend beyond the hinge axis or through compensating fins, suitably calibrated. They are generally used on gliders and small aircraft, but they were widespread before the advent of the fastest and most performing jet aircraft. Over time, the increase in aircraft mass and speed has made it necessary to switch to different forms of primary flight controls, namely enhanced controls.

The enhanced controls mainly utilize hydraulic systems, controlled by a global hydraulic installation or, more recently, by small hydraulic stations located near the flight control, in order to reduce inertias and weights involved. Lately, electromechanically implemented flight controls are beginning to be spread, with the aim, in the future, to supplant hydraulics. Consequently, it is possible to trace an evolutionary profile of flight controls: initially, the reversible flight controls provided a direct connection between the cabin controls and the aerodynamic appendages, using cables or levers. With the increase in the number of surfaces, the hydraulic controls were introduced, for which the cabin controls indirectly operate the appendages, acting on valves and hydraulic devices. With the advent of the electronics, these commands have become "active", meaning that they are able to operate continuous corrections and interventions on the aerodynamic appendages, independently of the pilots' action. On the latest combat aircraft, the absence of electronics would prevent control. In fact, the on-board computers help the pilot, assisting the commands given with hundreds or thousands of micro-movements per second. The last frontier of the commands for aerodynamic appendices is that of the use of fly-by-wire technologies (with copper wiring) or fly-by-light (with optic fiber cables).

From this examination, we can observe a "removal" of the pilot from the direct control of the aerodynamic appendages: this means that the pilot's muscle strength is no longer imparted directly to the flight control, but, due to the great forces at stake, it is necessary to have a servo assistance. The control surfaces of a Boeing 747 or A380 would require dozens of people to be moved!

The servo-controls, therefore, not only allow to operate surfaces that would require very high forces, but also allow to automatically perform the balancing of the flight control. By balancing we mean the maintenance of the government surface with zero incidence with respect to the axis of the wing or the elevator. On the other hand, this implies that the enhanced flight controls must be able to give feedback to the pilot when he performs high

load factor¹ and/or high-speed maneuvers. For this purpose, appropriate artificial sensitivity systems intervene, which allow to return the sensation of the maneuvers performed to the pilot. In other words, at high speed and high load factors the pilot will receive a reaction in the form of "heavier" flight controls. This is a protection for the aircraft itself that, therefore, cannot be brought to its extreme limits in an unconscious way by the pilot.

It is possible to draw a conceptual scheme, shown in Figure 2, which explains how the enhanced flight controls work. This diagram shows the closed-loop logic between the moving surfaces, the signal sent to the flight controls and the power command, necessary for their movement. This logic, implemented in an on-board computer, helps the pilot to steer the aircraft, to allow fully automatic control by appropriate navigation systems.

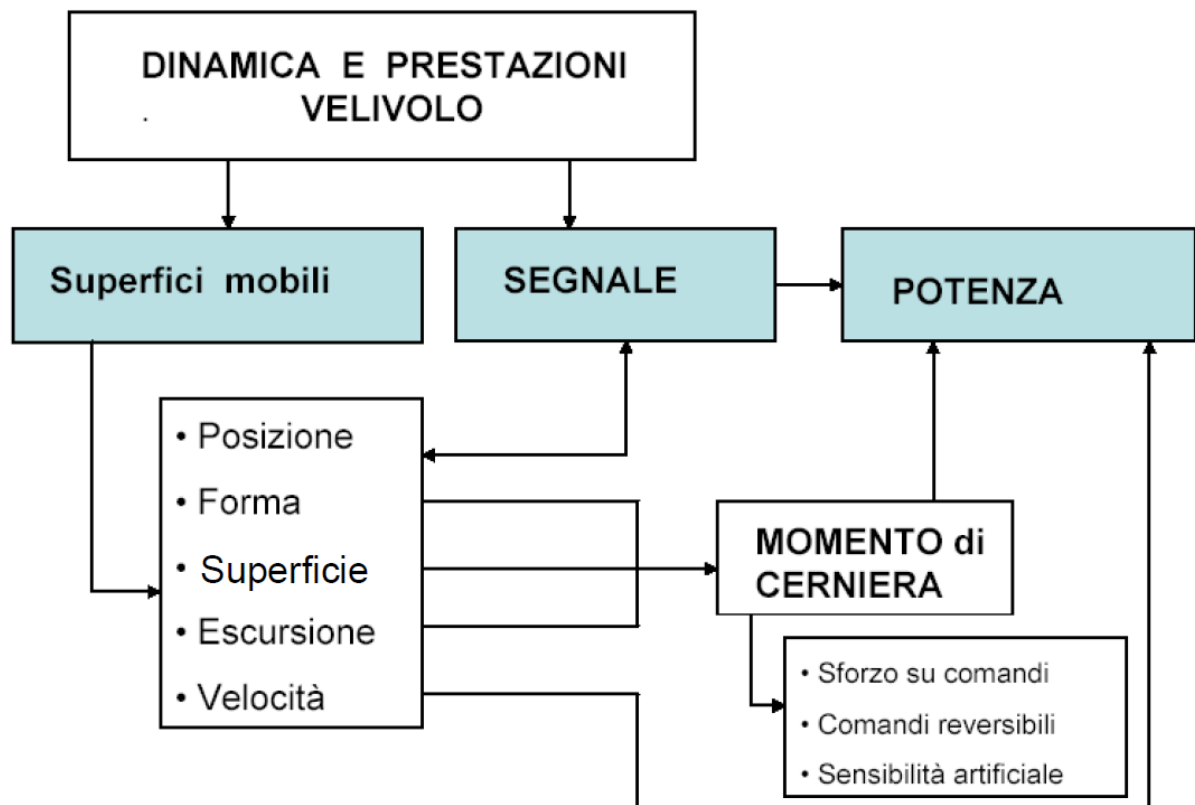


Figure 2 Conceptual scheme of enhanced flight controls

¹ By load factor we mean the ratio between the lift and the weight of the aircraft. During maneuvers that involve an abrupt change of attitude, this factor tends to increase strongly, resulting in a high stress on the structures of the aircraft. The regulation establishes, therefore, the maximum load factor limit that each class of aircraft must bear to be certified

We can also identify some advantages of enhanced flight controls compared to reversible flight controls:

- Greater stiffness, with locked controls, of mobile surfaces, or limited deflection of the moving surface, when this is subject to external loads, with the pilot keeping the control element still.
- With free controls, for example when the pilot leaves the control bar, the mobile surfaces are not free to float, but are brought to a neutral position, under the call of the artificial sensitivity system.
- There is no longer any need to compensate for the aerodynamic forces, since the forces that move the surfaces are exerted by specific actuating organs (electric or hydraulic); this means that the flight surfaces are "cleaner", more rational and lighter.

To compensate for the natural tendencies of an aircraft to deviate from the trajectory imposed by the pilot due to possible imbalances in the calibration of the surfaces of government, there are systems to compensate for these imbalances, which take the name of "trim". In the case of reversible flight controls, the "trimming" action takes place through suitable surfaces (called "trim tabs"). On the other hand, on more complex and advanced airplanes it is possible to exploit the constructive flexibility of the primary flight surfaces, to act directly on the balancing of the flight attitude, without the need for dedicated appendages. This is the case of the use of fractional flight surfaces, on airplanes like the Airbus A380.

1.1. Primary and secondary flight controls

Figure 3 shows the different surfaces of an aircraft, whose position can be changed through the use of flight controls.

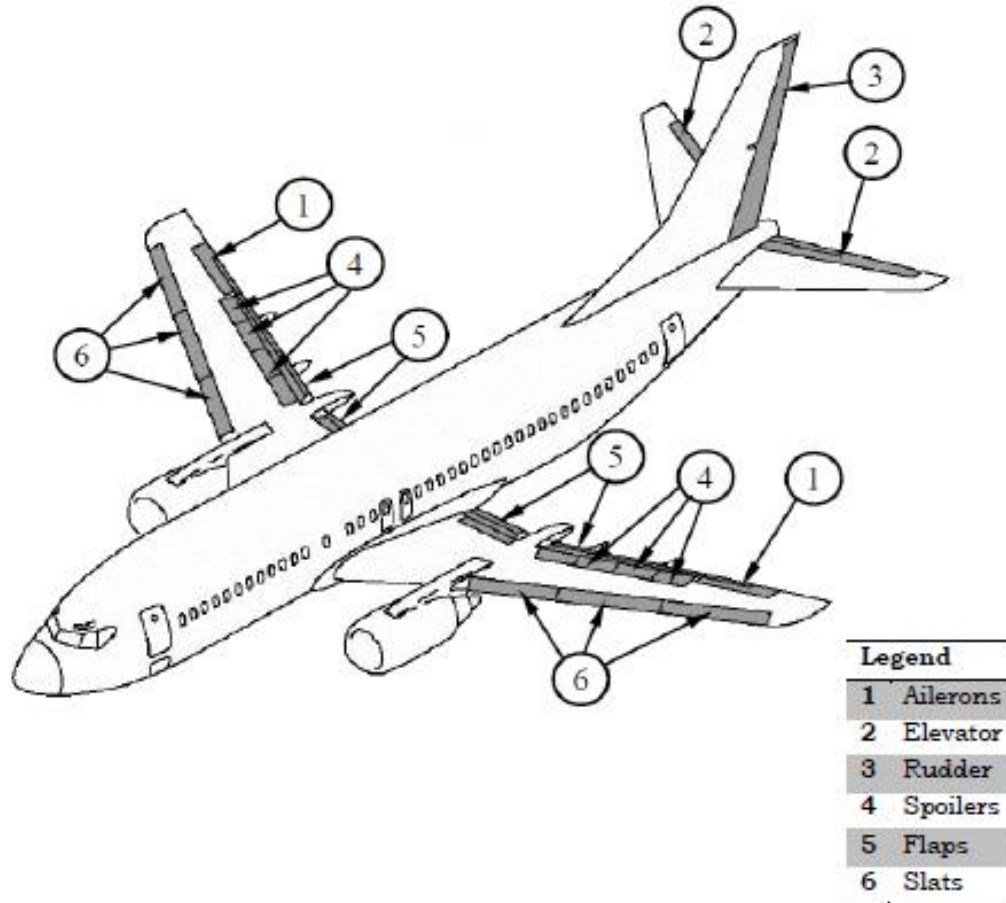


Figure 3 Control surfaces of an airliner

The primary flight controls control the three axes of the aircraft:

- Roll, managed by the ailerons (elements 1 in Figure 3), which generates a moment around the longitudinal axis of the aircraft (x axis). They are operated conjugally but antisymmetrically.
- Pitching, managed by the elevator (element 2 in Figure 3), which generates a moment around the transverse axis of the aircraft (y axis). Generally, the elevator is divided into two surfaces, operated conjugally and symmetrically.
- Yaw, managed by the rudder (item 3 in Figure 3), which generates a moment around the vertical axis of the aircraft (z axis).

Secondary flight controls are operated sporadically during specific flight phases. They are intended to change the attitude or speed of the aircraft. The main ones are:

- Spoilers (item 4 in Figure 3), which have the purpose of increasing the aerodynamic drag and can assist the ailerons in the turning phase, if operated in an antisymmetric way.
- When the spoilers are operated in unison, they become airbrakes (again item 4 of Figure 3).
- Flaps (elements 5 and 6 of Figure 3), whose purpose is to increase the aircraft's lift coefficient in the take-off and landing phases or during low speed maneuvers. In the landing phase, their total extension allows to increase the resistance coefficient to contribute, in part, to slow down the aircraft.

2. Actuation Systems

On commercial or military aircraft currently in use, flight controls are usually hydraulically or electrically operated: for the primary controls, in general, hydraulic expansion is used, with linear cylinder-piston motors or (very rarely) linear motors; the secondary controls, on the other hand, can be made using hydraulic or electric rotary motors.

In the last decades, basically following the development of reliable electric motors (with a high power/weight ratio) and the consolidation of the necessary technologies, secondary electromechanical controls have established themselves in the field of small powers (typically < 7 kW) and, even with due caution, they begin to find practical uses also for the implementation of primary commands, especially in the field of UAVs and small aircraft. This will allow, in the future, to completely replace the hydraulic power with the electric one, which for now is starting to take hold in actuators of the EHA (Electro-Hydraulic Actuator) and EBHA (Electro-Hydraulic Backup Actuator), where the electric motor drags directly the spool instead of the flapper nozzle or jet pipe systems.

The actuation systems, which can be used to measure almost all physical quantities (such as speed, force, pressure, position, temperature or electrical quantities), are intended to measure their output and, if necessary, to change it quickly and precisely. In these systems, therefore, the output of an actuator is compared to the command sent to the system. Based on the difference between these two signals, an input is sent to the controller, which has the purpose of varying the input and output signal of the actuator. This process can be explained with the diagram shown in Figure 4.

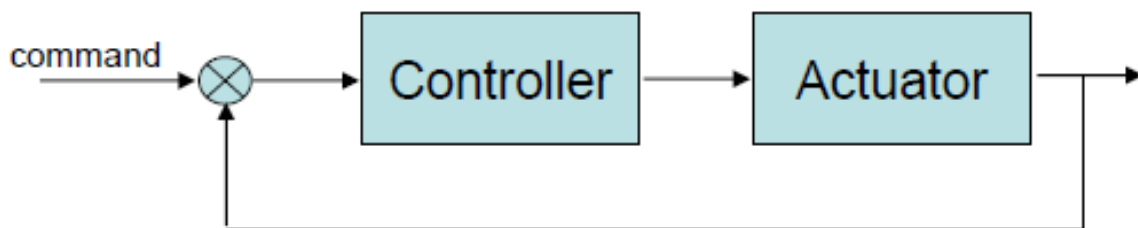


Figure 4 Control scheme of an actuation system

The difference between the input supplied to the system and the output of the actuator defines the performance of the entire system.

Figure 5 shows possible solutions in use, all rotary, of the screw-nut and ball screw type, which could be characterized by gears, but also ball or roller screw systems.

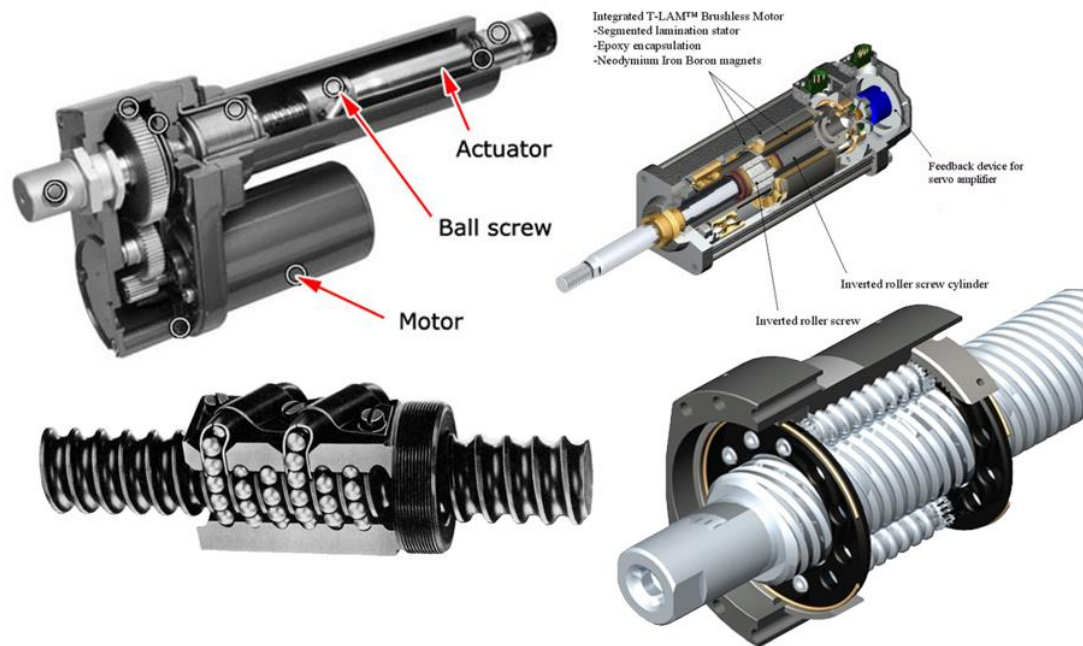


Figure 5 Rotary actuators with screw-nut system and with ball screw system

There are four main actuation systems, which will be explained below:

- Hydromechanical actuation systems
- Electrohydraulic actuation systems
- Electrohydrostatic actuation systems (EHA)
- Electromechanical actuation systems (EMA)

2.1. Hydromechanical Actuation Systems

Hydromechanical servomechanisms use a double-acting jack system. The delivery and return lines are always connected through levers to the controls in the cabin and, by a system based on the use of areas, allow to guarantee the multiplication of the human force applied on the controls, transferring it to the control surfaces of the aircraft.

Therefore, they utilize the elementary principles of oleo-dynamics to multiply the force exerted in points even far from the control cabin. An appropriate mechanical feedback system allows to give the pilot the feeling of the applied command entity ("artificial sensitivity"). The diagram of the servomechanism described is shown in Figure 6.

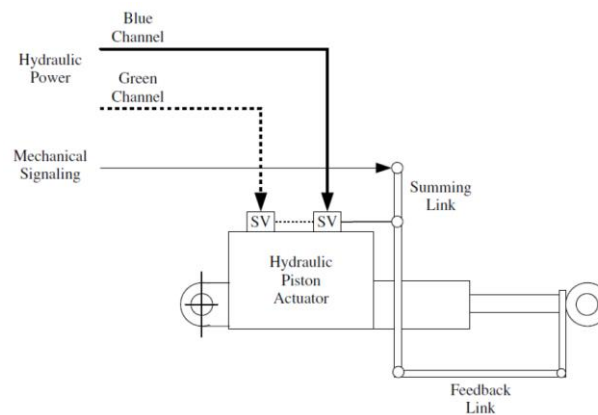


Figure 6 Diagram of a conventional hydromechanical servomechanism

Since hydraulics is a "filter" between the human force and the aerodynamic action, it is possible to introduce rudimentary systems of automatic piloting (as shown in Figure 7), through electric actuators, connected to the physical lines of feedback.

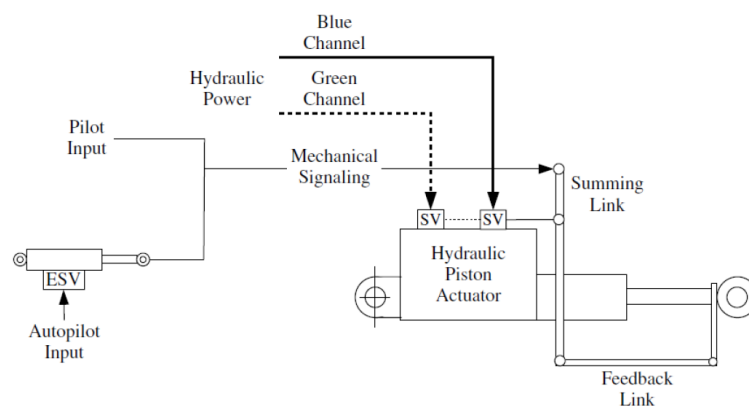


Figure 7 Diagram of a hydromechanical servomechanism with electric autopilot

In summary, the cabin controls act on the valves that control the jacks, enhancing the action of the pilot.

2.2. Electrohydraulic Actuation Systems

The electrohydraulic servomechanisms make use of hydraulic lines spread all over the aircraft, controlled by variable displacement axial piston pumps, driven by constant rotation electric motors. The pump flow rate defines the speed at which the controls are operated.

In Figure 8 the scheme of this mechanism has been reported.

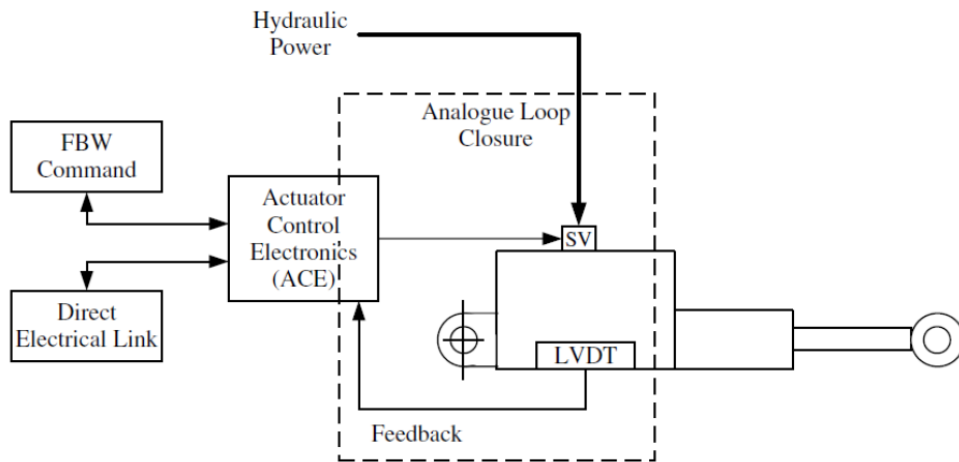


Figure 8 Diagram of an electrohydraulic servomechanism

The electro-hydraulic servomechanisms make use of different types of valves, designed to control the movement of the jacks connected to the control surfaces. Those valves could be:

- Flapper nozzle: a thin blade, called "flapper", dispenses the flow of oil between two chambers, which are able to generate an overpressure capable of deforming the flapper and causing the displacement of the spool. What comes to the nozzles is a very small fraction of the flow rate of the circuit and the small diameter of the nozzles themselves requires a micrometric filtration of the oil. The flapper is driven by a torque motor, which deflects according to the current received by two magnets, which induce a torque capable of flexing the flapper. A representation of this kind of valve can be seen in Figure 9.

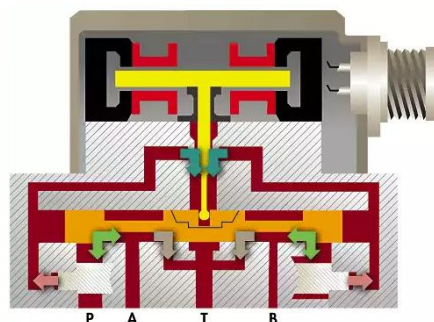


Figure 9 Flapper nozzle valve

→ Jet pipe: compared to the previous case, a torque motor of a bigger entity directs a suitable flow of oil into two opposite chambers, capable of causing the spool to move due to the received overpressure. In this case, an oil flow is not diverted, but the efflux channel is appropriately oriented (the jet pipe, in fact). Compared to flapper nozzles, jet pipe valves have better performance and save some of the acquisition costs, since it is not necessary to include in the sales cost the royalties required for the use of the other technology. A representation of this valve can be seen in Figure 10.

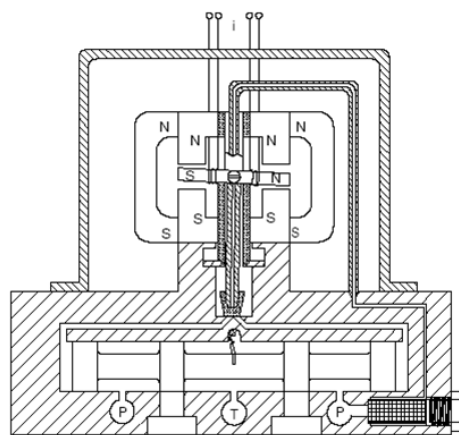


Figure 10 Jet pipe valve

→ Jet deflector: instead of having a moving nozzle, rotated by a torque motor, a deflector, which directs the flow where required, is placed downstream of the nozzle. Given the greater compactness of the system, better dynamic performances are obtained, which result in a much more reactive control of the system.

→ Direct Drive Valves (DDV): these valves allow to eliminate the system based on torque motor or jet, since the spool is moved directly by a dedicated electric motor. They are the last frontier in the field of servovalves. A representation of this kind of valve can be seen in Figure 11.

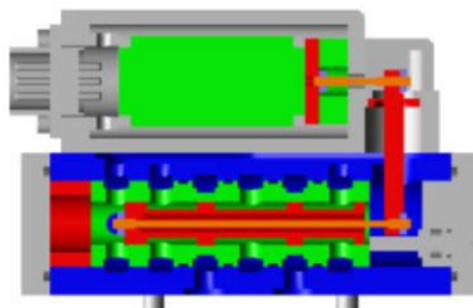


Figure 11 DDV valve

Since the implementation also involves an electronic part, it is possible to obtain very high quality controls, capable of reacting much more quickly to the inputs of the pilot. At the same time, all automatic commands (such as, for example, the autopilot) are more precise and effective.

This type of servo-controls is well suited for use in fly-by-wire or fly-by-light systems, where an appropriate sensor system provides adequate feedback, both to the pilot and to the aircraft control systems. It can therefore be said that hydraulics is a pure vector generated by the actions of the pilot.

2.3. Electrohydrostatic Actuation Systems (EHA)

In order to simplify, lighten and compact the hydraulics of modern aircraft, whose dimensions and performance tend to increase more and more, the electrohydrostatic actuators have been introduced. In this case, the hydraulic system of the aircraft is reduced to a minimum and is no longer widespread within the entire aircraft. In fact, in correspondence of the commands to be moved, an integrated system is created, consisting of an electronic control unit, which commands a variable speed motor in feedback; the motor actuates a constant displacement pump. By means of this pump, a hydraulic jack is actuated. This jack is connected in closed loop to the on-board computers of the aircraft through suitable sensors.

Thanks to the electro-hydrostatic actuators, it is possible to make the action on the controls even more prompt and dynamic, preserving the artificial sensitivity returned to the pilot.

A diagram in which the connections to the various on-board control units are noted, is provided in Figure 12.

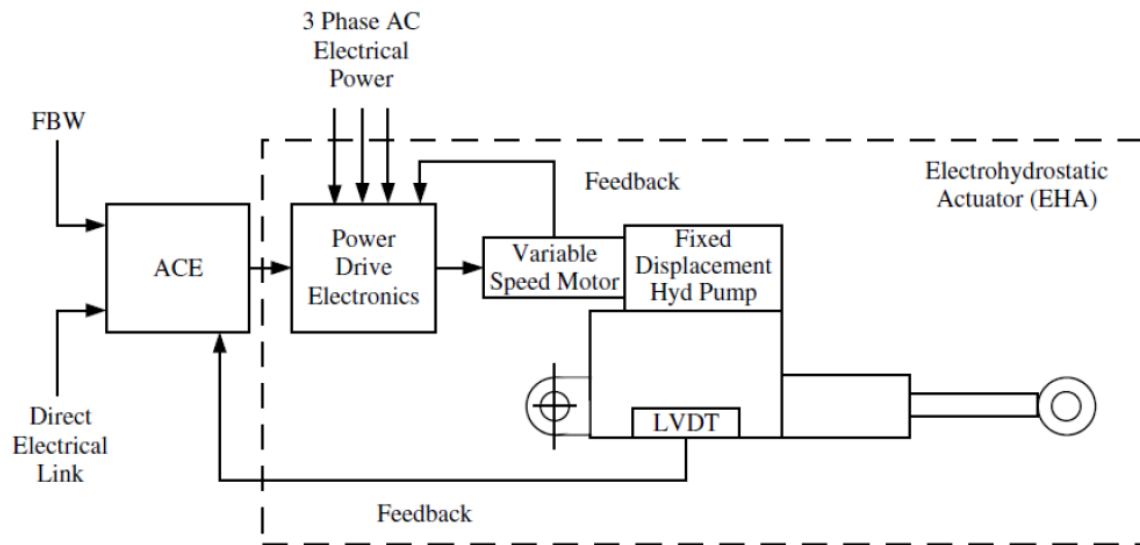


Figure 12 Scheme of an EHA

2.4. Electromechanical Actuation Systems (EMA)

Electromechanical actuators are the final evolution and the future trend in flight controls. To push the weight savings and the compactness of the system to the extreme consequences, the control electronics of the command acts, through power and control signals, on an electric motor, connected in closed loop to the control unit itself.

The motor is then connected via a reduction gear to a screw-nut or ball screw system. Finally, the screw-nut or ball screw system is connected to the flight control by an appropriate mechanical connection.

The movement signal of the actuator is constantly monitored by appropriate sensors, whose feedback is sent to the on-board computer of the aircraft. This type of actuator allows to reduce weights and dimensions, as well as to further improve the responses of the aircraft to the commands given by the pilot or the computer itself.

Thanks to the greater safety achieved by electrical and electronic components, it is possible to reduce the weights and dimensions of the appropriate redundancy² systems required in any aerospace system.

The scheme of an EMA system is shown in Figure 13.

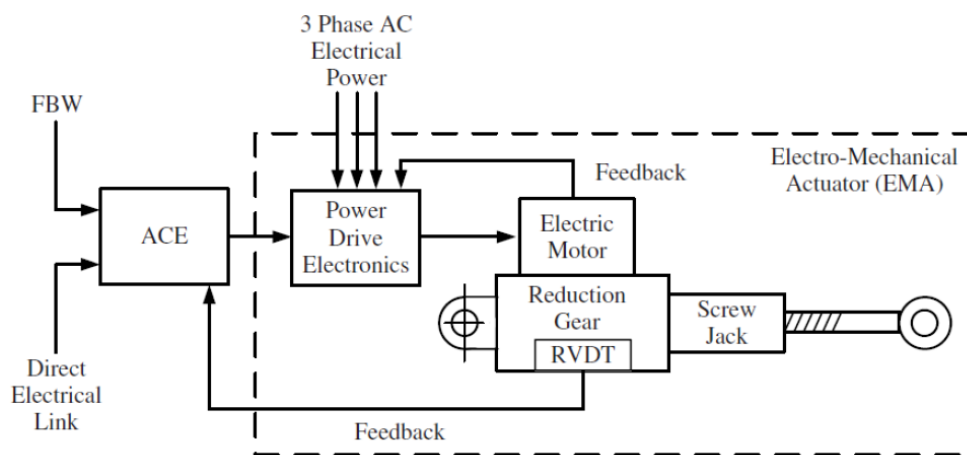


Figure 13 Scheme of an EMA system

The aim of this thesis is that of designing and constructing the conceptual prototype of the epicycloidal reduction gear, used as a component of the test bench of an EMA.

² In the aeronautical field, it is defined as "redundant" any system whose functionality can be appropriately multiplied, in order to guarantee the correct and continuous operation of the system itself, in the moment in which a part of it not working correctly. For example, in the case of a hydraulic system, the aircraft will be equipped with at least two or three independent systems (depending on the size of the aircraft itself), capable of substituting one of those systems, in case of failure

3. Fused Deposition Modeling

3.1. Technology

The development of prototyping technologies over the years has led more and more towards the birth of technologies that allow to obtain prototypes in a short time, with the most precise structures possible and also obtaining complex shapes, but always at affordable costs. For this reason, additive manufacturing techniques for polymers are an important resource for the prototyping industry, given the high flexibility of the machines that can be used, as well as the simplicity in the use of design and process management software.

The most common additive manufacturing technique for desktop printers is Fused Deposition Modeling (FDM). This technique is based on the fusion and subsequent deposition on a plane of a wire made of thermoplastic polymeric material, to obtain, through the superposition of successive layers, the finished piece.

The FDM processes are flexible, but not very precise and, therefore, impose limits regarding the internal finishing and the mechanical resistance of the parts produced. Despite that, this type of technology is of great interest in the field of prototyping and for the creation of molds for lost-wax casting, thanks to the low cost of the machines and materials used.

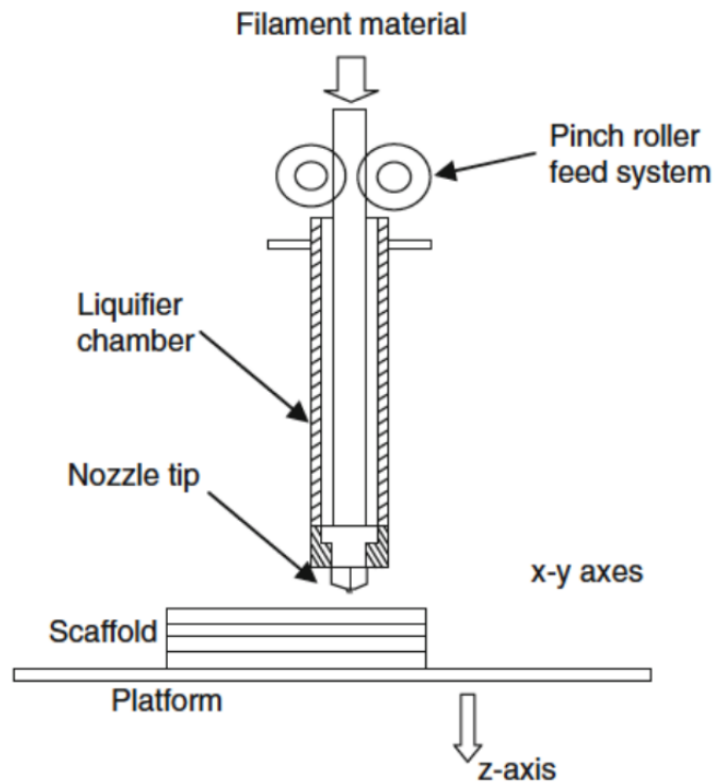


Figure 14 System for the fusion and deposition of the material for FDM

In Figure 14 a simplified scheme of the fusion and deposition system of the material for FDM has been reported. The process consists of three main steps:

- 1) Some gears push the polymeric filament downwards, making it pass through a heated channel.
- 2) The polymer is melted along the heated channel and sent to the nozzle.
- 3) The nozzle extrudes and deposits the polymer; the deposition head generates a pressure on the wire, enough to obtain the deposition of the wire itself on the work surface.

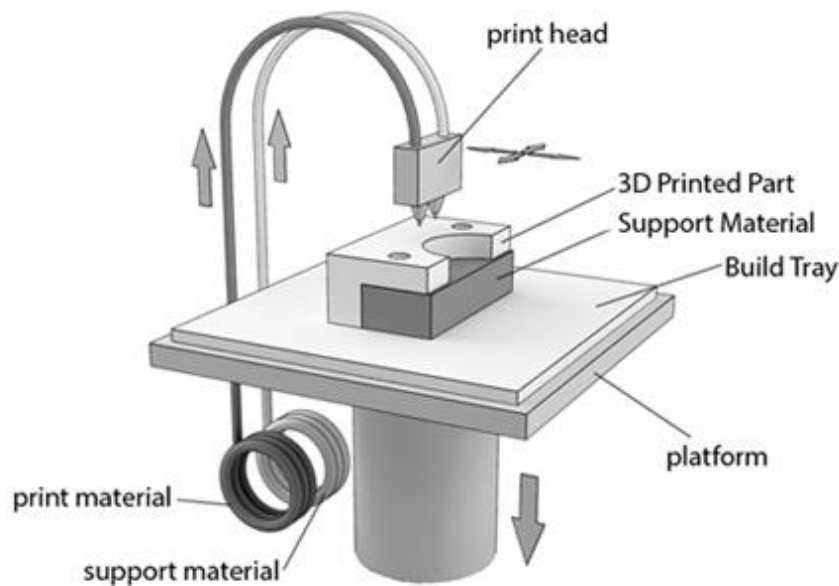


Figure 15 Movements in a machine for FDM

Figure 15 shows how the main movements inside the FDM machines are the motion of the nozzle on the xy plane, which allows to manage the deposition of the wire in the desired areas for the single section, and the movement of the deposition plane on the z axis direction, which allows to pass from the deposition of a layer to that of the next. The fact that the material is deposited in layers causes the presence of anisotropy inside the final component. The individual sections on the xy plane will therefore have higher mechanical properties than those found along the z axis. This aspect must be considered during the orientation of the piece in the machine.

The deposited polymeric material must have a slightly higher temperature than the melting temperature of the material itself. In this way, the molten wire has the characteristics necessary to be able to "glue" to the previously deposited layer and to solidify immediately thereafter.

Given the temperatures at which the material is deposited, another source of irregularity in the final structure obtained may be the formation of liquid or gas inside the component.

In the first case, if the extrusion temperature of the wire is excessive, there is the risk of obtaining a final structure made of an internal zone not completely solidified with an external "crust". The final structure, therefore, could be particularly weak, even for prototyping applications.

In the second case, the deposition of gas in the voids can occur. This may not have any negative effect in terms of strength of the final component, if the voids are on the external surfaces, as only the surface finishing gets worse. If, on the other hand, the gas infiltrates inside the part produced, it can generate tensions within the finished component. These tensions reduce the mechanical strength of the component produced and cannot be reduced with a subsequent heat treatment, which would only increase the risk of creep.

These two negative effects can be limited by managing the machine parameters. To limit the presence of liquid it is necessary to work at a temperature which is closer to the melting temperature, while to limit the presence of voids and the infiltration of gas it is advisable to make sure that the nozzle displacement speeds are not excessively high.

3.2. Materials

The number of materials that can be used for FDM is limited, as the technique requires the use of thermoplastic polymers. The main characteristic for a material, so that it can be used for extrusion, is that it must be easily spinable, thus it can take the shape of a wire, with a diameter between 1.4 mm and 8 mm. According to what previously said, the most used materials for this technique are ABS, PLA and PVA.

3.2.1. ABS (Acrylonitrile Butadiene Styrene)

ABS is a polymer used for a large variety of applications. Its mechanical properties depend on the percentages of the functional groups that compose it and, depending on the structure obtained, it is possible to produce elements such as the bumpers or the dashboard for cars, pipes or components for electronics.

This polymer is easily customizable, based on what has just been said, and among the materials available for FDM is the one with the best mechanical characteristics. In fact, it has a good flexibility and a good resistance to heat. Table 1 shows the characteristics of the material, considering the variety of ABS structures supplied by the company Stratasys.

	ABS	ABSi	ABSplus	ABS/PC
Tensile strength	22 MPa	37 MPa	36 MPa	34.8 MPa
Tensile modulus	1.627 MPa	1.915 MPa	2.265 MPa	1.827 MPa
Elongation	6%	3.1%	4%	4.3%
Flexural strength	41 MPa	61 MPa	52 MPa	50 MPa
Flexural modulus	1.834 MPa	1.820 MPa	2.198 MPa	1.863 MPa

Table 1 Mechanical properties of the different types of ABS offered by Stratasys

Between the polymers shown in Table 1, the most critical is the one given by the compound of ABS and PC (Polycarbonate). This material is obtained by mixing two components, whose melting temperatures are very different. Consequently, during the printing phase it will be particularly important to pay attention to work in a temperature range that is in common between that of ABS and the one of PC, which must be extruded at much higher temperatures.

ABS must be extruded at high temperatures (the highest for the polymers described in this chapter), so the machines which are able to use this material work in the range between 210-250 ° C, while the maximum operating temperature of the components produced is 80 ° C.

The negative aspect of this material is the fact that during printing it releases harmful, carcinogenic fumes. It will not be possible, therefore, to use ABS for the project described in this thesis, if not using a closed chamber machine and with a system of toxic fumes disposal and filtering, which makes the machine that has to be used particularly expensive.

3.2.2. PLA (Polylactic Acid)

This thermoplastic polymer derives from renewable resources such as sugar cane, tapioca roots and potato or corn starch. For this reason, PLA is the best solution in terms of environmental impact, compared to ABS and PVA. It can therefore be used for applications such as dentistry and other medical applications and food packaging.

It is a biodegradable material, so, as opposed to ABS, it has almost zero disposal costs and does not generate residual toxic fumes, but only a sweetish smell. The only toxic element of PLA can be the dye, rather than the material itself.

Normally, the machines which use PLA are made to work at temperatures between 160°C and 220°C, so it is enough to heat the nozzle less than what is needed for the deposition of ABS. Moreover, to favor the obtaining of better final properties it is recommended to use a heated deposition plane (generally at 40-60°C) and, since the PLA has a lower heat dispersion, therefore a slow cooling, usually the machinery to process this material has a fan, which speeds up the decrease in temperature.

After the cooling, PLA is hard and brittle, so it has properties that make it suitable for prototyping applications or creating objects that are not overly stressed.

	PLA
Tensile strength	26 – 45 MPa
Tensile modulus	2.539 – 3.039 MPa
Elongation	1 – 2.5%
Flexural strength	45 – 84 MPa
Flexural modulus	2.470 – 2.930 MPa

Table 2 Mechanical properties of the PLA, obtained from the Stratasys datasheets

Table 2 shows the main mechanical characteristics for the PLA sold by the company Stratasys. From the data obtained it can be verified how the polylactic acid is more rigid than the ABS, with a lower elongation at break.

Given the ease in finding the material, in addition to the fact that it does not cause emissions of toxic fumes, PLA is the material that was chosen for the subsequent realization of the conceptual prototype of the reduction gear. Among the objectives of the design, therefore, there will also be that of structuring the assembly in such a way as to minimize the loads on the components of the assembly, where possible.

Another advantage of the PLA is the fact that it is a rather inexpensive material, given that a coil of black PLA 3D Italy (the material used to produce the components) has a cost of 35 €/kg.

3.2.3. PVA (Polyvinyl Alcohol)

PVA is a water-soluble thermoplastic polymer. It is used for applications such as the production of adhesive sheets, coating films (for example, transparent film) or for children's games, such as slimes.

It is a very flexible material and is extruded at a temperature of around 190°C. Usually PVA is used in FDM for the creation of support structures, when multi-nozzle machines are used (as will be explained in the following paragraphs), since being water-soluble it becomes easy to remove at the end of processing.

The high affinity with water means that PVA is much simpler to dissolve than PLA. Therefore, this polymer requires storage in a dry environment or in a sealed container and must be dried before use, so as not to jeopardize its usefulness during printing. Furthermore, being easily soluble, PVA is not suitable for the production of components exposed to weathering.

This material has a high cost and is very difficult to find, therefore it has not been used for printing the supports for the parts produced for this thesis. Another limitation to the use of this material derives from the fact that the printer used is a single nozzle one, so it would have been technically impossible to extrude both the PLA and the PVA at the same time.

3.2.4. Other materials

In addition to ABS, PLA and PVA, there are several new generation materials on the market, which allow to obtain specific characteristics. None of these has been used for the production of the components of the reduction gear, but it is right to mention them to complete the list of the materials available.

Here are some examples of these materials:

- Nylon 6 and Nylon 12 are ductile, flexible and tough, they must be extruded at high temperature (up to 265°C for Nylon 6 and up to 280°C for Nylon 12); moreover, they confer high mechanical characteristics to the components.
- TPU (Thermoplastic Polyurethane) is transparent and with high resistance to corrosion, abrasion and shear stresses.
- PC (Polycarbonate) is transparent, impact-resistant and has low thermal shrinkage; it is the only material that has been considered as an alternative to PLA for printing the components of the reduction gear, later discarded due to the high self-lubricating feature of the filament, which makes it difficult to print.
- Materials with characteristics similar to some components found in nature, such as wood (Laywood), marble (Sculpture), glass (T-Glase) and sand (Laybrick Sandstone).

3.3. Machine

The machines used for FDM can have different sizes, depending on the purpose of use.

The systems used can be distinguished between industrial systems, which generally cost more than € 50000 and are used for more complex applications (such as functional prototyping, rapid tooling, rapid casting and rapid manufacturing), and conceptual modelers, which are used for conceptual prototyping and generally cost less than € 50000.

Furthermore, a distinction can be made between single nozzle machines and multi-nozzle machines.

Single nozzle machines are less expensive and easier to handle, as they can only process one material at a time. The simplicity of management also derives from the fact that the operations needed to substitute the material are quick and easy.

Multi-nozzle machines, on the other hand, are more complex to handle, since the behavior of the two different materials must be taken into account during processing. The advantage, however, is that of being able to use a soluble material for the construction of the supports, which are elements with purely structural functionality, used to support projecting parts at an angle of less than 50-60° from the deposition plane. It is therefore possible to obtain more complex pieces with this type of machine.

Multi-nozzle printers generally use PVA for the generation of support structures, because thanks to its high solubility in water, it is easy to remove once the component has been printed. Usually, the removal of PVA requires an aqueous solution containing 20 g of NaOH for each liter of H₂O, kept for a few hours at a temperature of about 70°C.

For the production of the components shown in this thesis, a desktop printer (therefore a conceptual modeler) FabTotum Core Pro 2018, single nozzle and open chamber was used. This is the reason why neither PVA, nor ABS could be used. Moreover, a careful redesign has been made for the elements that would have required internal supported structures.



Figure 16 FabTotum Core Pro 2018 machine

The machine (shown in Figure 16 FabTotum Core Pro 2018 machine) has a heated deposition plane, an important element for the distension of the components during printing, since the processed material is PLA. A fundamental characteristic for the machine used is the simplicity of use, as the software for the management of the printing profiles provided by the manufacturers allows a vast amount of controls to adjust the parameters of the machine, before and during processing..

For the production of the pieces for FDM some basic steps are necessary, all managed through a PC connected to the machine used:

- 1) Design and generation of the CAD file.
- 2) Generation of the .stl file using a CAD software. STL stands for Standard Triangulation Language and indicates that the CAD file, once finished, is saved as a system of triangles, of which the coordinates of the three vertices and the orientation of the normal vector to the surface of the triangle are known. The saved model, therefore, is of "shell" type and can be processed with the program for the preparation of the piece for additive manufacturing.
- 3) Workpiece orientation in the machine, generation of support structures and slicing. The software Cura by Ultimaker is used; Cura reads the .stl file and, according to the settings provided, generates the support structures where needed. The final result is a file with a .gcode extension, containing the data of the piece to be processed and the instructions for the machine (nozzle movement speed, filling, wall thickness ...).
- 4) Construction of the piece with the FDM machine.
- 5) Post-processing, if necessary, which includes the removal of the supports and a finishing, if needed.

3.3.1. Software Ultimaker Cura

Cura, of the Ultimaker company, is the software designed to read the .stl file and to elaborate step 3 described in the previous paragraph.

With this software it was possible to manage the parameters of the machine and the orientation of the built piece, as well as the phase of application of the supports, where necessary, and of subdivision of the component into layers. Once selected the size specifications of the machine used (in our case, a volume of 177.8x177.8x300 mm), the .stl file generated by Solidworks can be loaded, resulting in a first view of the piece to be produced. Subsequently, the component shift and rotation commands can be used to obtain the desired position and orientation. An example is shown in Figure 17.

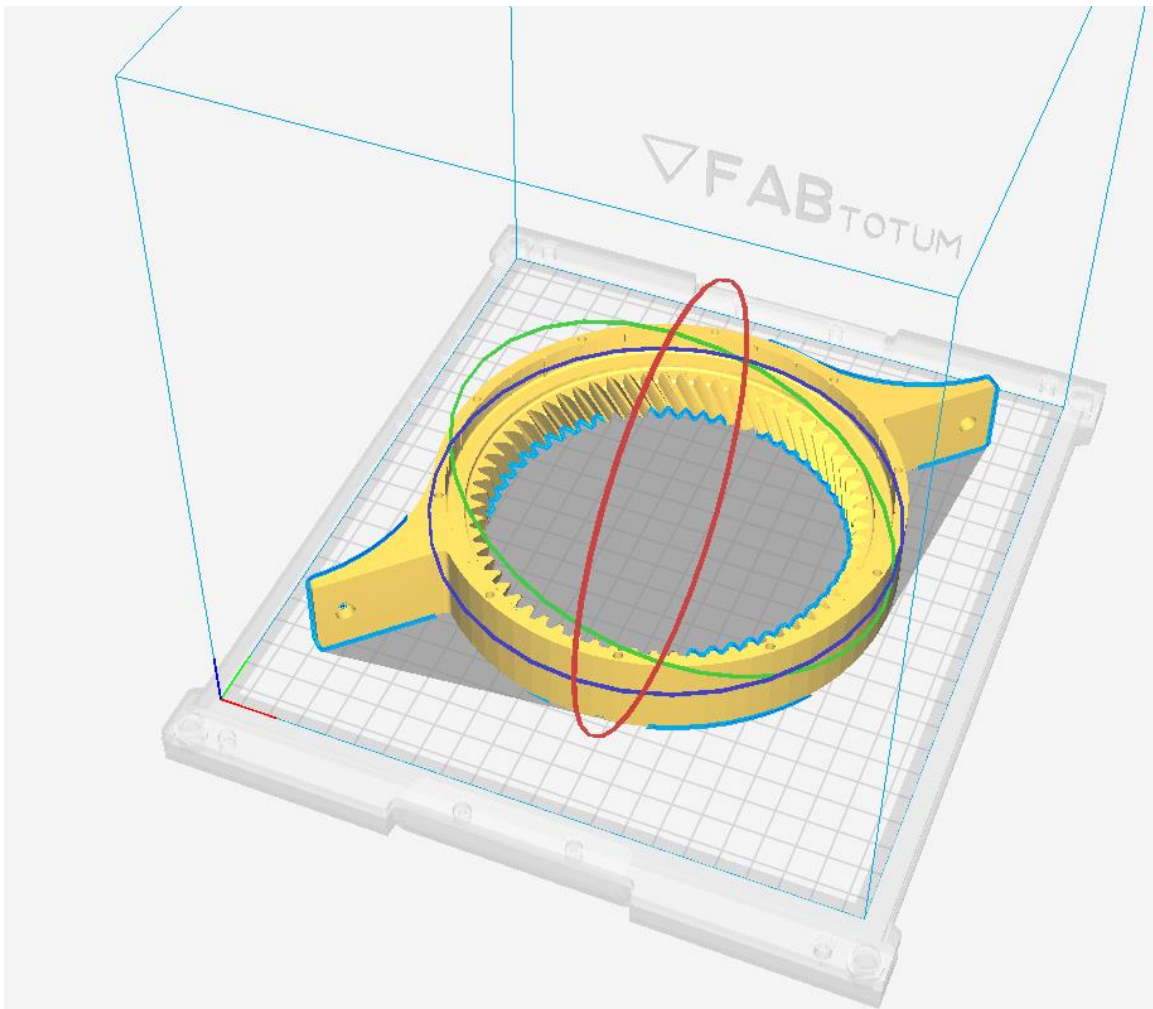


Figure 17 Example of a view of one of the produced components, once loaded into the Cura software

Afterwards, it is necessary to switch to parameter management. For the production of the components of the assembly, the setting of the layers defined as "Normal" has been used; this setting gives the layers a thickness of 0.15 mm. Cura offers a list of functions that allow to manage some fundamental parameters, such as the thickness of the first layer, the thickness of the filling lines and the thickness of the walls of the piece.

In Figure 18 the setting used for all the parts of the assembly has been reported.



Quality		
Layer Height		0.15 mm
Initial Layer Height		0.2 mm
Line Width		0.4 mm
Wall Line Width		0.4 mm
Outer Wall Line Width		0.4 mm
Inner Wall(s) Line Width		0.4 mm
Top/Bottom Line Width		0.4 mm
Infill Line Width		0.4 mm
Skirt/Brim Line Width		0.4 mm
Initial Layer Line Width		100.0 %

Figure 18 Settings used to manage the quality of the elements that make up the pieces produced

Furthermore, it is possible to manage the properties of the outer layers, such as the thickness of the walls and the lower layer, as well as the possibility of inserting a layer at a higher level than the last one, to improve the surface finishing of the piece. From Figure 19 we can see how the number of lines that make up the walls is obtained by dividing the wall thickness by the thickness value of the lines that make up the walls (namely, the wall line width):

$$Wall\ Line\ Count = \frac{Wall\ Thickness}{Wall\ Line\ Width} = 2.5$$

The software approximates this value by default, so the number of lines that make up the walls is two. For the upper and lower areas, walls of four layers were used. Thicker walls make it possible to have a more compact component, but can cause greater stresses, as well as requiring more material.

For the construction of the components of the reduction gear, it was not considered appropriate to produce layers at higher level than the last one set by the software.

Shell	
Wall Thickness	1 mm
Wall Line Count	2
Outer Wall Wipe Distance	0.2 mm
Top Surface Skin Layers	0
Top/Bottom Thickness	0.6 mm
Top Thickness	0.6 mm
Top Layers	4
Bottom Thickness	0.6 mm
Bottom Layers	4
Top/Bottom Pattern	Lines
Bottom Pattern Initial Layer	Lines

Figure 19 Settings used to manage the thickness of external layers

Another setting that can be managed using the software is the one relating to the infill. As in the case of the thickness of the outer layers, a greater infill can increase the effect of internal stresses on the piece produced, in addition to increasing the expense of material. For this reason, for large components, but with small internal volumes compared to the overall size of the piece, it was preferred to use the settings shown in Figure 20, with a 5% infill density. In the case of the production of large pieces, subjected to more substantial stresses, more importance has been given to the generation of thicker walls, rather than to an increase in internal density.

Pieces with lower volumes subjected to greater stress, such as gears, have a 24% infill density. With FDM it is not convenient to produce solid pieces with a 100% infill density.

Infill	
Infill Density	5 %
Infill Line Distance	16.0 mm
Infill Pattern	Grid
Connect Infill Lines	<input type="checkbox"/>
Infill Line Directions	[]
Infill X Offset	0 mm
Infill Y Offset	0 mm
Infill Line Multiplier	1
Infill Overlap Percentage	10 %
Infill Overlap	0.04 mm
Skin Overlap Percentage	5 %
Skin Overlap	0.02 mm

Figure 20 Infill settings for the pieces produced

As already mentioned, the material used for the production of the components is PLA, a material that requires extrusion at a temperature between 160°C and 220°C. Following numerous attempts, the nozzle temperature selected for printing is 195°C. This value has been considered the best in order to have a good surface finishing, obtainable at lower temperatures, since the material requires less time for cooling and reaching the final shape, and in order to avoid nozzle malfunctions, since the wire may not have sufficient sliding, if the nozzle works at too low temperatures.

Moreover, as shown in Figure 21, Cura software offers the possibility to manage the machine build plate temperature, the flow of extruded material through the nozzle, the printing speed and the speed of the "no-load" nozzle movements, which are the movements made by the nozzle when it is not extruding material to generate the workpiece.

Material			Speed		
Default Printing Temperature	↻	195 °C	Print Speed	↻	30 mm/s
Printing Temperature		195 °C	Infill Speed	↻	50 mm/s
Printing Temperature Initial Layer		195 °C	Wall Speed		30 mm/s
Initial Printing Temperature		195 °C	Outer Wall Speed		20 mm/s
Final Printing Temperature		190 °C	Inner Wall Speed	↻	40 mm/s
Default Build Plate Temperature	⊗ ↻	50 °C	Top/Bottom Speed		15 mm/s
Build Plate Temperature	⊗	50 °C	Support Speed	⊗	30 mm/s
Build Plate Temperature Initial Layer	⊗	50 °C	Travel Speed	↻	150 mm/s
Flow	↻	95 %	Initial Layer Speed		22.0 mm/s
Initial Layer Flow		95 %	Skirt/Brim Speed	⊗	22.0 mm/s

Figure 21 Settings for temperature and extrusion speed

The temperature of the deposition plate has been set at 50°C. This setting allows to reduce the residual stresses in the component being printed; too low temperature values may not have a positive effect on the process, while too high values risk to excessively delay the definitive cooling of the material, causing the rise of more imperfections or the deformation of the job, if it gets removed from the plate immediately. We must bear in mind the fact that the heating of the deposition plate mainly affects the first layers and less and less with the progress of printing, since the nozzle deposits the material in areas farthest from the plate itself.

In the "Material" section of the software it is also possible to choose the flow of extruded material through the nozzle. Reducing this parameter to a value below 100% makes it possible to obtain a better surface finishing, as it decreases the tendency of the nozzle to deposit excess material in areas where the infill value is higher (this is, therefore, referred to walls of the pieces produced).

The printing speed manages the movement speed of the extrusion head in the areas where the material is to be deposited. A too low value of this parameter causes an increase in the production times of the job, while a too high value could jeopardize the functioning of the nozzle. The nozzle, in fact, must respect a maximum flow limit of material that can be deposited (which is the flow value that the nozzle can supply when the corresponding parameter is brought to the value of 100%).

If the speed of movement of the head exceeds that of extrusion, there is the risk of not being able to deposit the material, which is not heated in time and tends to form a cap that obstructs the nozzle. If this happens, the printing operations must be interrupted, the piece produced must be removed and thrown away (as the machine does not allow to recover the process data from the point where it was interrupted), the material must be removed and the filament must be loaded again in the print head; only at this point the process can be restarted. All these operations involve a huge waste of time and material, which is why the search for the right combination of nozzle speed parameters and material flow has been the subject of the analyzes carried out, before being able to move on to the production of the pieces that make up the reduction gear.

The final combination obtained for the two parameters is given by a flow of material of 95%, with the print head moving at a speed of 30 mm/s. This combination, therefore, allows a lower use of material, working at the maximum printing speed allowed by the nozzle (which is the one recommended to the machine manufacturer). The maximum speed allowed, in fact, is 50 mm / s, and has been assigned by the software to the production speed of the infill lines. The print speed value, therefore, is a function of this parameter and has been researched iteratively, until having all the parameters described in Figure 21 below the maximum allowed value. It can also be noted that the minimum print speed is the one assigned to the initial layers (22 mm/s); this precaution guarantees a better adhesion of the material to the deposition plane.

The speed of travel, however, allows a wider choice. The only factor that must be taken into account is the deposition of residues by the nozzle in areas where it is not necessary to extrude the material because the print head, before starting the movement, retracts the material for 2.5 mm inside nozzle (as shown in Figure 22), to reduce residues in the displacement areas. If the speed of travel is low, the risk is to increase the residues released by the nozzle in these areas, as the material starts to flow again before the nozzle has reached the new printing area. If the displacement speed is too high, the nozzle tends to not yet have available material to be deposited in the new printing area. To reduce working time, the maximum displacement value recommended by the machine manufacturers was assumed. This value is 150 mm/s.

Retraction Distance	2.5	mm
Retraction Speed	23	mm/s
Retraction Retract Speed	23	mm/s
Retraction Prime Speed	23	mm/s

Figure 22 Distance and speed values of retraction of the material

The deposition head has a cooling fan, which allows to speed up the reduction of the temperature of the material (advantage already anticipated when describing the PLA). In this case, no parameter adjustment was performed, keeping the airflow at 100% and following the parameters provided by the manufacturers (shown in Figure 23).

* Cooling	
Enable Print Cooling	<input checked="" type="checkbox"/>
Fan Speed	100.0 %
Regular Fan Speed	100.0 %
Maximum Fan Speed	100.0 %
Regular/Maximum Fan Speed Threshold	10 s
Initial Fan Speed	0 %
Regular Fan Speed at Height	0.2 mm
Regular Fan Speed at Layer	2
Minimum Layer Time	5 s
Minimum Speed	20 mm/s

Figure 23 Cooling fan management parameters

The software would make it possible to have a difference between the air flow for the layers with a printing time lower than a defined value and the air flow for the layers with a printing time exceeding this defined value. In this case, however, the function has not been utilized.

Management of support areas was of great importance. In the example shown in Figure 24, the supports were added only where they could be in contact with the printing bed. The internal protruding areas, therefore, have not been supported, because they have a re-entry of a few tenths of millimeter.

The value of the inclination angle, set at 65°, allows the software to automatically insert the support structures only in the areas with an angle from the deposition plate lower than the one defined. Moreover, the "zig zag" structure used is the easiest to remove, a very important feature, as the supports of the same material of the piece are often complex to remove and their removal can damage the final component. Even the low density value of the support structures (10%) constitutes an additional factor that guarantees the simplicity of removal of the supports themselves.

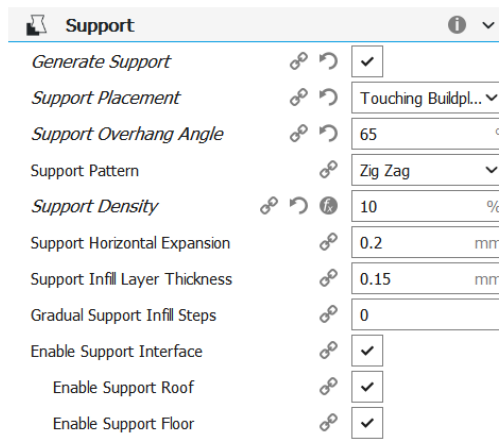


Figure 24 Assigned values for the generation of support areas

Once all the print parameters of the component have been defined, the Ultimaker Cura software generates a preview, which shows a view of the finished component in the machine, allows analyzing the structure of the individual layers, as shown in Figure 25, and shows an approximate value of the printing time (for the component shown, 9 hours and 45 minutes).

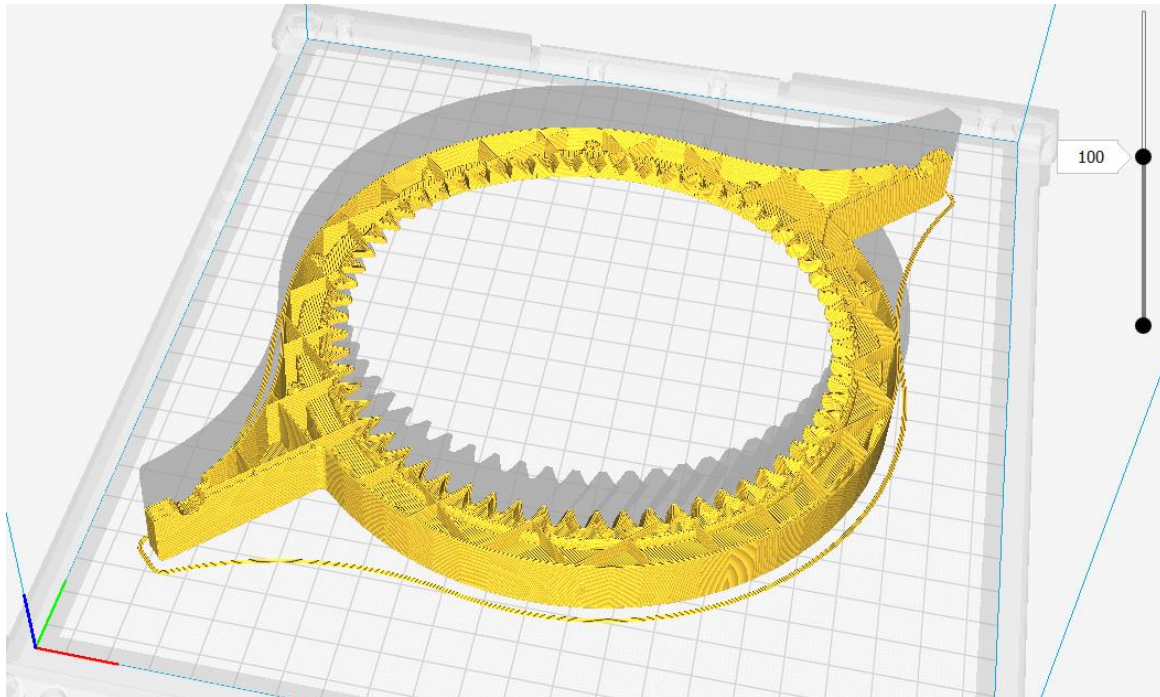


Figure 25 Example of preview of the component divided into layers

Once checked the generation of the support structures and the correct division into layers, the component can be saved. The software generates a file with the extension .gcode, which contains all the parameters described in this paragraph, in addition to the data of the print head path and the information on the shape of the component itself..

3.3.2. FABUI application

Once the .gcode extension file is obtained, the process can be managed using the application provided by the machine manufacturers: FABUI software, an application that can be used by using any browser on the PC connected to the machine via ethernet cable.

This application allows to manage project folders by inserting the .gcode files to be reproduced.

When using the machine for the first time, it is generally recommended to calibrate the printing bed, which allows to level the height and inclination of the surface on which the material is deposited, so as to reduce inaccuracies that can be managed without having to necessarily change the parameters of the machine.

After calibration, once the plane has been cleaned, the first piece can be printed.

The application allows to monitor in real time the nozzle temperature and the temperature of the deposition plate and, if necessary, allows to interrupt the process. Figure 26 shows the user interface during the printing processes performed to produce the reduction gear.

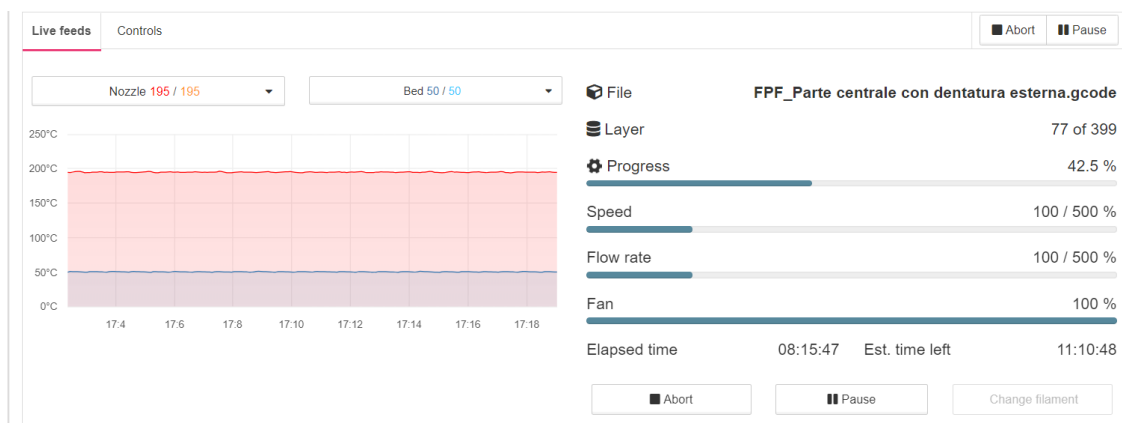


Figure 26 FABUI interface during the printing process

Moreover, through the controls shown in Figure 27, it is possible to manage these two temperatures, the speed of the print head, the flow of material and the air flow of the fan. Moreover, the controls allow to manage a possible vertical displacement of the plane, if necessary.

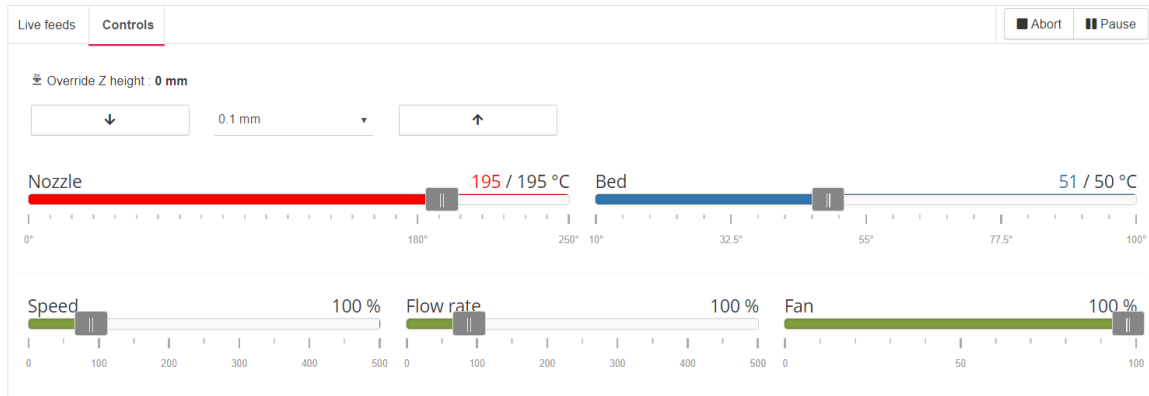


Figure 27 Controls provided by the FABUI application

4. Production of the functional prototype of the reduction gear

4.1. CAD design and production conditions for FDM

The production of the reduction gear starts from the generation of the CAD file (shown in Figure 28), obtained by designing the pieces as if they were to be produced by traditional manufacturing.

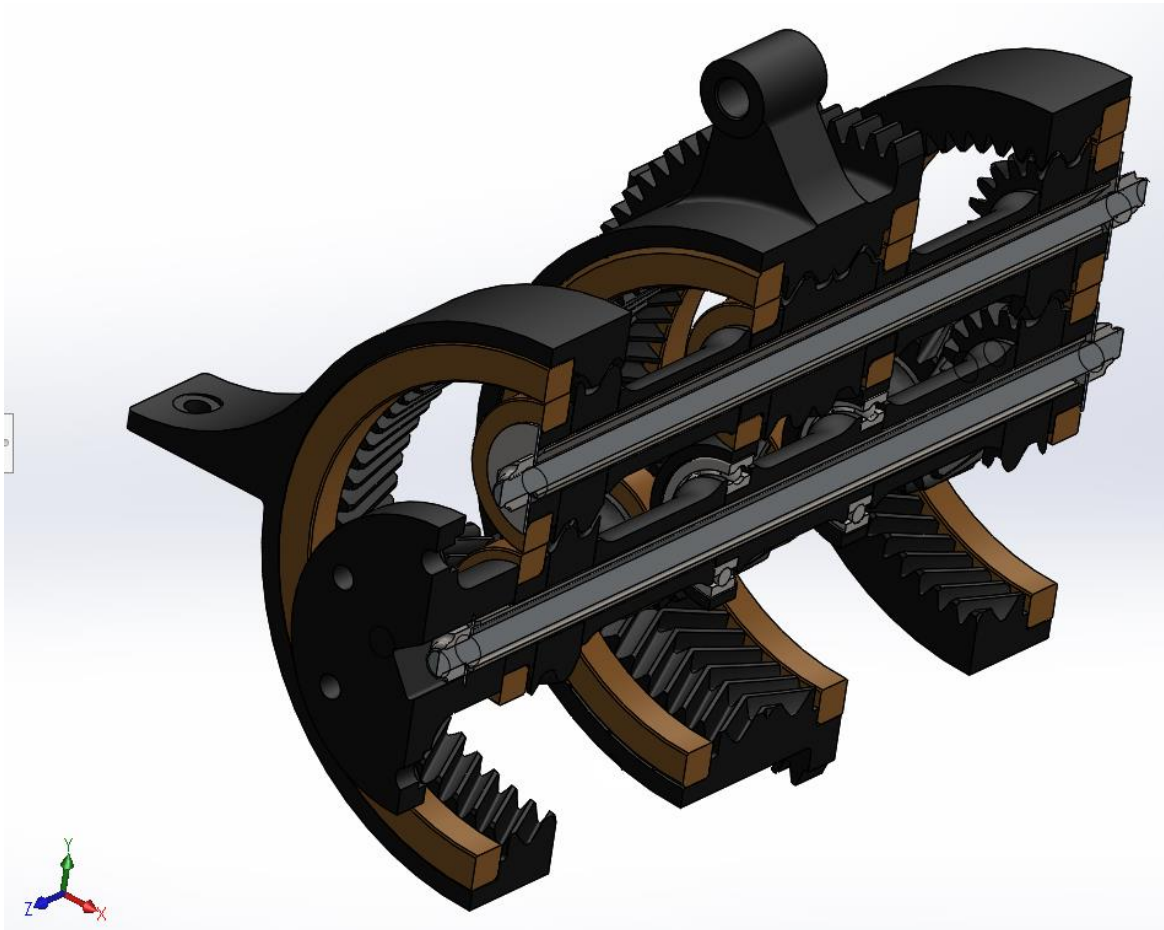


Figure 28 Section of the reduction gear to be produced for Additive Manufacturing

The CAD shows that the reduction gear is made of four shafts (initially with a circular section) and three internal gears.

The central shaft is defined as "solar gear" and is composed of three spacers, two gear wheels with a specular toothing angle and an adapter for the connection to the electric motor.

The three external shafts are called "planetary gears" and are composed by two spacers and three gear wheels (shown in Figure 29): two with a specular tothing angle and one, the central one, double-helical, to balance the axial forces in a more effective way.

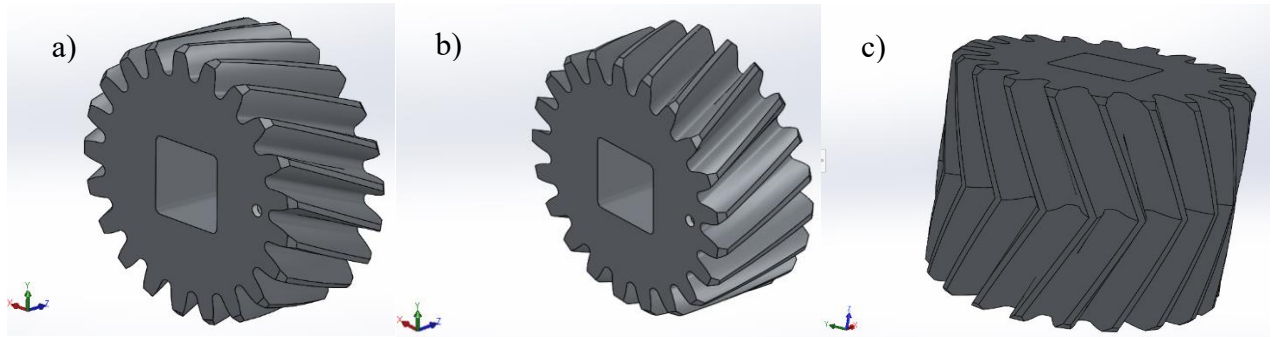


Figure 29 CAD model of gear wheels: gear wheel 21l (a) and gear wheel 21r (b), with specular tothing angles, and gear wheel 20 (c), double-helical

While no redesign was required for rings and spacers (but just a reduction of the outer diameters of 1 mm), the design of the gear wheels involved special attention, as printing via FDM requires respect for some fundamental constraints.

The main conditions to be met are the following:

- it is not possible to produce protruding surfaces for more than 2-3 mm; therefore, it is necessary to redesign the components that have protruding surfaces with dimensions greater than the indicated value which, otherwise, would require the generation of supports
- the supports cannot be used, except on sections having at least two opposite sides communicating with the outside or for protruding surfaces of sufficiently high dimensions; the machine used for FDM has a single nozzle, therefore the supports are more difficult to remove if they do not respect this constraint, since they are produced with the same material as the one used for the component
- the holes created must have a dimension greater than 2 mm, because for smaller dimensions the material tends to fill the hole itself
- where it is possible, the inclination of the surfaces must be greater than 60° , in order to avoid the addition of support structures, which are difficult to remove
- the dimensions of the pieces produced must take into account an error between 0,5 mm and 2 mm (value obtained experimentally); consequently, the individual pieces of the assembly drawn with the CAD software must be corrected before each print, so as to take into account this error, to obtain a final piece whose dimensions are as close as possible to those of the original project.

The last error described, that is the dimensional error, is due to the effect of the thermal shrinkage of the job being printed. The deposited material is affected by the difference in temperature between the outlet of the nozzle and the external environment (being the chamber of the printer partially closed and not completely closed). This results in a constriction of the component. Furthermore, the shrinkage is proportional to the size of the piece to be printed; the greater the diameter of the piece, the greater the effect of the thermal shrinkage.

The deposition plane, however, is heated, so it allows to limit the phenomenon and improve the properties of the finished piece in terms of mechanical resistance and finishing. The thermal effect, however, must be considered in the phase of resizing the pieces to pass from the nominal measures of the CAD file to the measures for the printing phase.

It is therefore possible to proceed to the study of the individual components, with a view to producing the assembly by additive manufacturing, following the constraints described above.

4.2. Reduction ratio

To be able to calculate the reduction ratio, which is the effect of the reduction in speed made by the reduction gear, we can refer to the diagram shown in Figure 30.

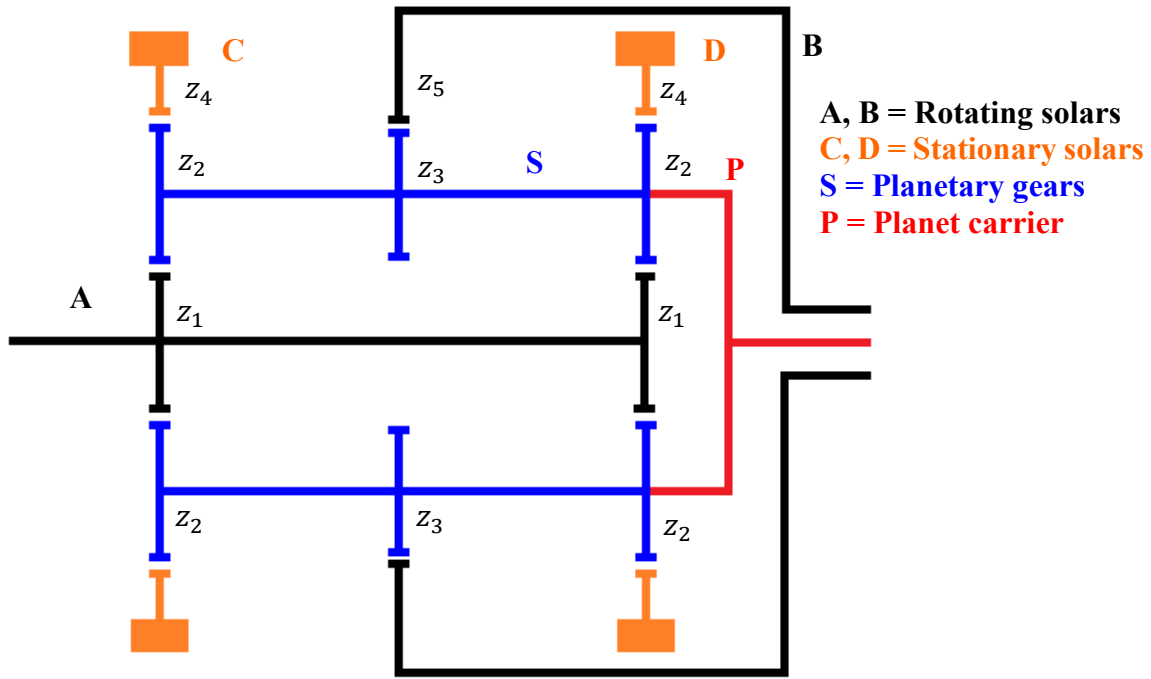


Figure 30 Diagram of the structure of the reduction gear

The reduction ratio was calculated with the following steps:

- 1) Calculate the angular velocity of the stationary solars C and D, considering the relative motion with respect to the planet carrier ($\tilde{\omega}_4$) and assuming the relative angular velocity of the rotating solar A ($\tilde{\omega}_1$) to be positive:

$$\tilde{\omega}_4 = -\tilde{\omega}_1 \frac{z_1}{z_4}$$

- 2) The absolute angular velocity of the stationary solars (ω_4) is zero, consequently:

$$\omega_4 = \tilde{\omega}_4 + \Omega = 0 \Rightarrow \Omega = -\tilde{\omega}_4 = \tilde{\omega}_1 \frac{z_1}{z_4}$$

- 3) It is now possible to calculate the angular velocity of the solar B, in relative motion with respect to the carrier ($\tilde{\omega}_5$):

$$\tilde{\omega}_5 = -\tilde{\omega}_1 \frac{z_1 z_3}{z_2 z_5}$$

- 4) Thanks to the equations obtained in the first three steps we can now calculate the absolute angular velocities of the rotating solar A and B:

$$\omega_1 = \tilde{\omega}_1 + \Omega = \tilde{\omega}_1 \left(1 + \frac{z_1}{z_4}\right)$$

$$\omega_5 = \tilde{\omega}_5 + \Omega = \tilde{\omega}_1 \left(-\frac{z_1 z_3}{z_2 z_5} + \frac{z_1}{z_4}\right)$$

- 5) From these last two equations, it is possible to obtain the reduction ratio between the input speed of the rotating solar A and the output speed of the rotating solar B, considering the number of teeth of the gear wheels that make up the reduction gear (z_1, z_2, z_3, z_4 and z_5):

$$\tau = \frac{\omega_1}{\omega_5} = \frac{1 + \frac{z_1}{z_4}}{\frac{z_1}{z_4} - \frac{z_1 z_3}{z_2 z_5}}$$

To simplify the calculation, the variables used to obtain the reduction ratio have been reduced to three. This was made possible by expressing the radius of the gear wheels of the stationary solar C and D (r_4) and the radius of the gear wheels of the rotating solar B (r_5) as a function of the radii of the gear wheels which make up the planetary gears (r_2 e r_3) and of the radius of the gear wheels which make up the rotating solar A (r_1), bearing in mind that the radius of a gear wheel is $r = \frac{mz}{2}$ and the modulus (m) is the same for all the gear wheels that make up the reduction gear:

$$r_4 = r_1 + 2r_2 \Rightarrow z_4 = z_1 + 2z_2$$

$$r_5 = r_1 + r_2 + r_3 \Rightarrow z_5 = z_1 + z_2 + z_3$$

Once the equations just described were obtained, to select the reduction ratio a simple Matlab script was used; this script calculates the reduction ratio, starting from the number of teeth of the wheels which make up the rotating solar A and of the wheels that make up the planetary gears. With the iterative procedure, the final result of the reduction ratio was obtained assuming $z_1 = z_2 = 21$ and $z_3 = 20$:

$$\begin{cases} z_4 = z_1 + 2z_2 = 63 \\ z_5 = z_1 + z_2 + z_3 = 62 \end{cases} \Rightarrow \tau = \frac{1 + \frac{z_1}{z_4}}{\frac{z_1}{z_4} - \frac{z_1 z_3}{z_2 z_5}} = 124$$

Analyzing the equations obtained, it is clear that, in order to obtain better reduction ratios, it would be sufficient to maintain constant the number of the teeth of the gear wheels that make up the planetary gears (z_2 and z_3), and, with a constant modulus, to reduce the number of teeth of the gear wheels which form the rotating solar A. For example, for a number of teeth of the gear wheels forming the rotating solar A reduced to 14, the overall reduction ratio increases to 165. However, for simplicity and higher production efficiency, the number of teeth of the gear wheels forming the rotating solar A has been kept equal to the number of teeth of the lateral gear wheels of the planetary gears (therefore, $z_1 = z_2$). Moreover, the hypothesis of using a number of teeth of 14 is not feasible, since the minimum number of teeth for gear wheels with tooth angle of 20° , with no correction to the tothing ($x = 0$), is:

$$z_{min} = \frac{2(1 - x)}{\sin^2(20^\circ)} \approx 17$$

Furthermore, the choice of the reduction ratio was based on the search for an integer, non-decimal value, which will make it possible to simplify the calculations on the measurements detected by the encoder, when it will be possible to perform the rotation tests of the reduction gear.

For planetary reduction gears, a constraint must be respected: the sum of the number of teeth of the wheels which form the solar A with the number of teeth inside the lateral internal gear must be divisible by the number of satellites. In our case, there are three satellites and the sum of the cogs quoted is 84, which is divisible by three. The calculations are therefore acceptable

It is now possible to proceed with the design and construction of the components that make up the reduction gear.

4.3. Analysis of the first gear wheel

For the production of the single pieces that make up the assembly, it is necessary to perform a test print on the models that would be produced by "traditional manufacturing", to analyze, subsequently, the criticalities that emerge in the production through additive manufacturing (namely, the parts of each component that do not respect the constraints listed in the previous paragraph). The aim is to redesign individual pieces, to facilitate production through FDM.

The first pieces analyzed are the gear wheels.

Each gear wheel requires the presence of two flanges, one on each side of the gear wheel itself. For the traditional manufacture, the wheel could be made "piece", that is obtained from the shaft of the planetary gear to which it belongs, producing the grooves with subsequent processing. This procedure is not possible with additive manufacturing.

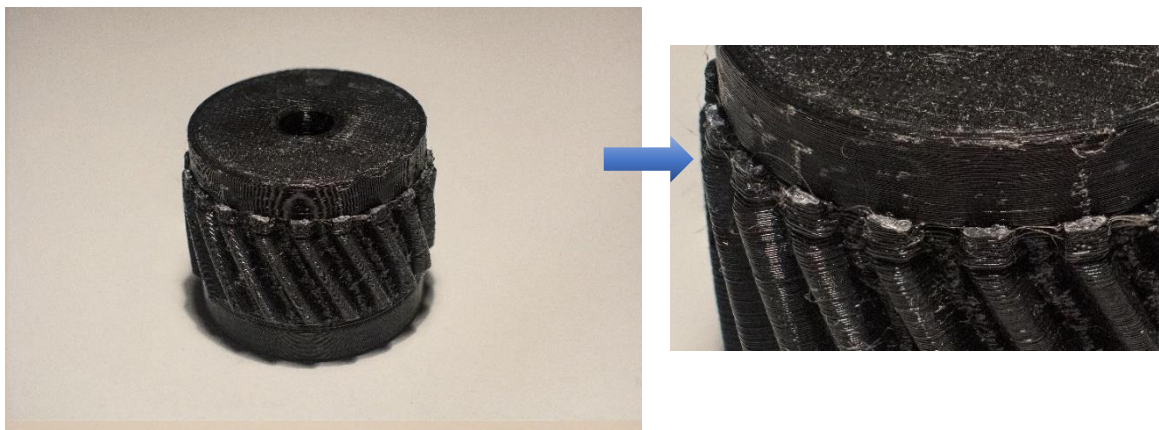


Figure 31 First printing of a gear wheel, without the manufacturing fixes for FDM, and detail of the support structures in the grooves

Figure 31 shows the result of the printing of the gear wheel without the corrections for production through additive manufacturing. It is clear how the support structures are filling the space between the teeth, as well as the space in the groove between the wheel and the flange, making it impossible to remove the support itself.

The result obtained is impossible to assemble, as well as requiring a high printing time.

A first redesign attempt, therefore, consists in removing the supports in the spaces between the teeth (increasing the minimum angle for inserting the supports, on the Ultimaker Cura software) and removing the grooves. This idea has been realized (as reported in Figure 32), but immediately discarded: the absence of the grooves makes it less easy the meshing between two adjacent wheels, making the eventual assembly phase impossible. However, the printing time is reduced by the absence of support structures, so it can be considered as a starting point for the next printings.



Figure 32 Gear wheel produced without grooves and internal supports

This last result has required a more drastic measure, that is to redesign the component, breaking it down into smaller elements to be coupled afterwards, to obtain the gear wheel structure drawn in the original CAD.

This solution will be considered only if the problems related to the production technique cannot be solved in any other way. In fact, although a redesign can shorten the subsequent printing times and solve any problems related to technology, it requires the development of a new problem analysis, usually making the need to perform new tests emerge (in this case new coupling tests). Therefore, it is necessary to evaluate the time needed for the redesign itself and for the validation of the new project obtained as part of the total printing time.

For simplicity and symmetry purposes, the wheel has been divided into three components: the two external flanges and the gear wheel.



Figure 33 Structure of the gear wheel divided into three components

This type of structure causes an increase in the total printing time, but allows to start the production of several pieces of the same type at the same time, giving the possibility to perform small productions in series. Furthermore, since the structure shown in Figure 33 has been designed for the purpose of carrying out tests that reproduce the final assembly and the meshing of the gear wheels in the reduction gear, the new configuration allows to repeat only the printing of the gear wheel once obtained the correct measurements for the production of the flanges. Therefore, the production time of the wheel itself is reduced.

The critical element of the new structure are the couplings between the flanges and the gear wheel; three cylinders protruding from the flanges (Figure 34) of 3 mm diameter, 4 mm high, were used, inserted in the cylindrical slots, obtained in the wheel.

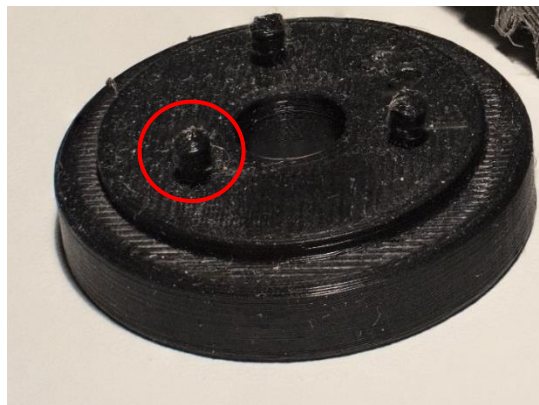


Figure 34 Detail of the cylinders used for the coupling of the flanges with the gear wheel

Studying these coupling elements allowed to obtain experimentally the error made by the machine, when used in the printing of small pieces. In fact, in order to be able to couple the cylinders with interference, it was necessary to obtain slots with a diameter of 4 mm in the gear wheel. The result was obtained through a "trial and error" procedure.

We can easily obtain the approximate radial error of the machine for elements with a diameter of less than 10 mm as half the difference between the nominal size and the one used for the slots:

$$error = \frac{d_{slot} - d_{cylinder}}{2} = 0.5 \text{ mm}$$

As already described above, the diametrical error increases as a function of the dimension of the elements to be coupled.

The new structure obtained allows a good repeatability and allows to perform the meshing tests, but the 3 mm cylinders are an element of weakness. Therefore, when designing the gear wheels for the assembly of the actual reduction gear, it will be necessary to think about a different type of coupling between wheels and flanges.

Furthermore, this first wheel structure has a cylindrical slot for inserting the gear wheels into a base which allows the meshing tests. This central structure must also be replaced for subsequent assembly of the reduction gear.

4.4. Meshing between two gear wheels

The purpose of the subsequent tests was to find the correct size of the teeth and the correct meshing distance of the gear wheels, so as to obtain a contact between the flanges of the two adjacent wheels. The aim is to obtain the condition visible from the CAD section shown in Figure 35.

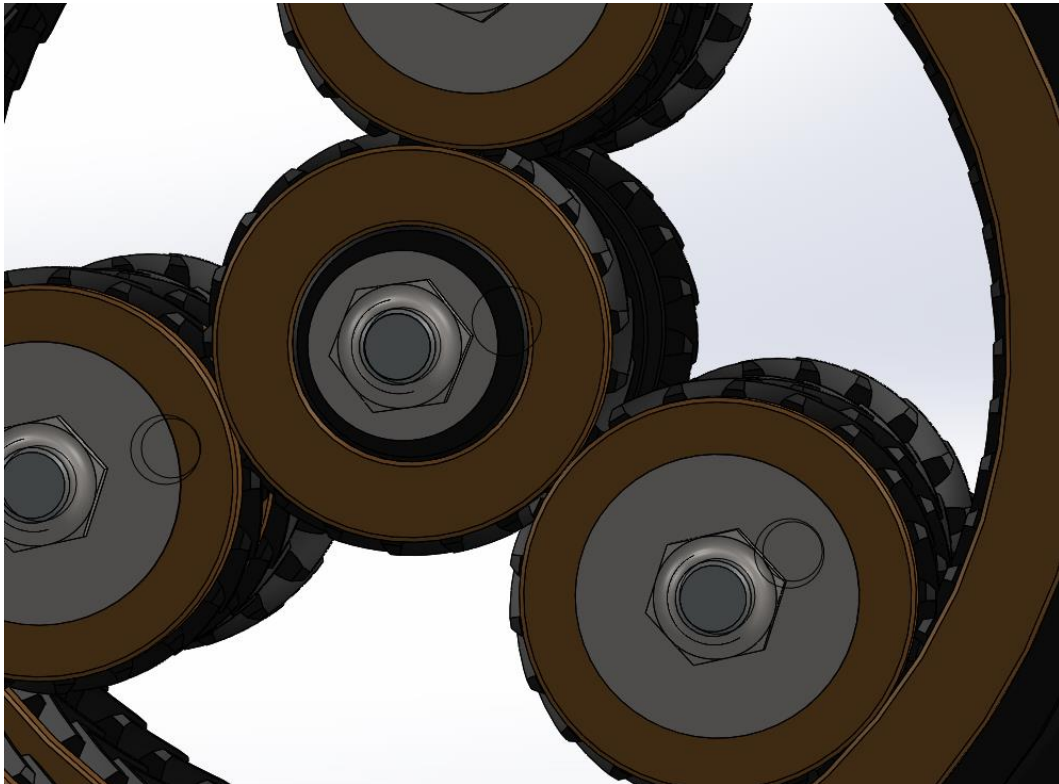


Figure 35 Contact between adjacent flanges in the final assembly

The analysis of the drawing shows how the function of the flanges is to unload the gear wheels by their radial load, while allowing a precise meshing condition.

The first step was to print the gear wheels with the project dimensions, which means considering an outside diameter of 44 mm, a root diameter of 34 mm and a tooth fillet of 0.5 mm. Figure 36 shows the gear wheels obtained and the components used for the test.



Figure 36 Gear wheels used in the first meshing test

The result of the meshing test made it possible to highlight the first criticality, which is the distance of about 2 mm between the two adjacent flanges. The objective of the next test, therefore, is to correct the root diameter and outside diameter, in addition to the width of the teeth, so as to have the contact between the flanges of two adjacent wheels.

To obtain the result of Figure 37, the following dimensions had to be used:

- Outside diameter of 43 mm
- Root diameter of 33 mm
- Tooth fillet of 1 mm



Figure 37 Second meshing test, to have contact between adjacent flanges

The test performed made it possible to obtain the contact between the two adjacent flanges but showed a second reason for criticality. The gear wheels have an excessive clearance, which does not allow the correct meshing. To solve this problem, therefore, it has been necessary to find the correct width of the teeth, so as to increase the accuracy in the contact between the teeth of the gear wheels.

In order to obtain a sufficient meshing precision, which does not compromise the constraint of maintaining contact between the two adjacent flanges, a value of the outside diameter intermediate between that of the first and that of the second test has been used. Therefore, keeping the root diameter constant at 33 mm and the tooth fillet at a value of 1 mm, the outside diameter was increased to 43.4 mm.



Figure 38 Final result of the meshing test, with contact of the adjacent flanges

With this last value used, the teeth mesh without clearance and the adjacent flanges remain in contact (as shown in Figure 38).

Moreover, Figure 39 shows the detail of the meshing between the adjacent gear wheels.



Figure 39 Detail of the meshing between adjacent gear wheels

Figure 40, instead, shows the measurements used in the CAD, thus obtaining the final structure of the gear wheels, from which it was possible to proceed with the design and construction of the first planetary gear. It is important to point out that the measures we are referring to will be those of the central wheels of the planetary gears, namely the double-helical ones. For the external wheels, which are single-helical, the measurements of the main diameters have been modified, referring to what has been obtained in this paragraph, taking into account the proportion ratio between the different wheels.

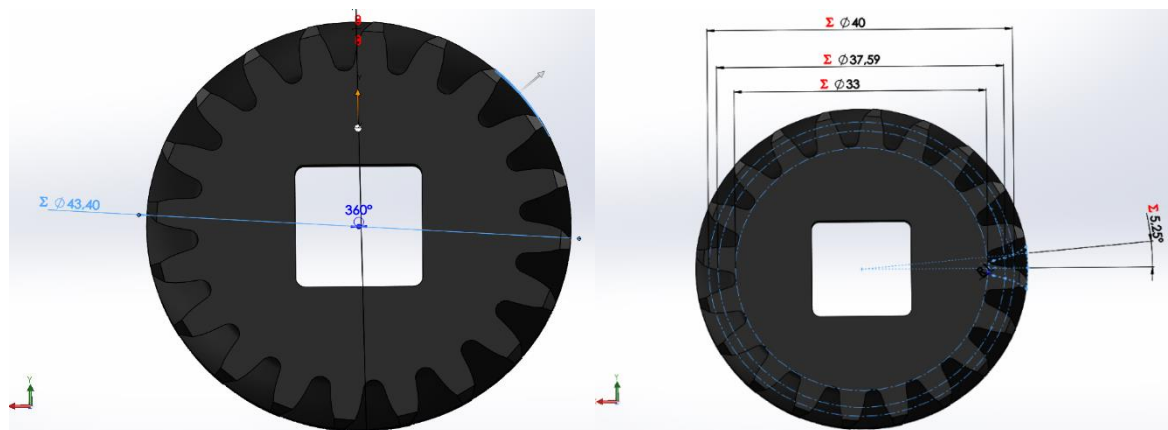


Figure 40 Final measurements of double-angle gear wheels

4.5. Assembly of the first planetary gear

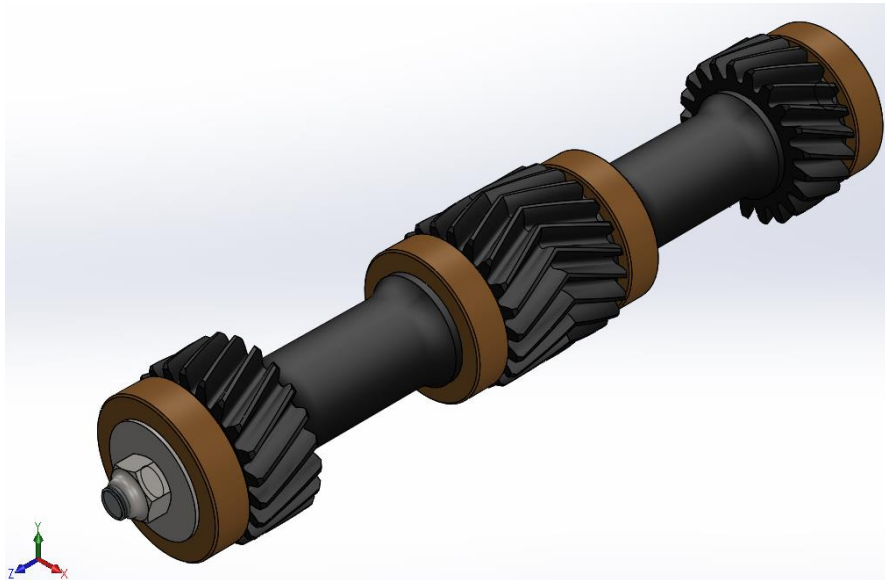


Figure 41 Assembly of the planetary gear, obtained from the CAD of the reduction gear

Figure 41 shows the design of the planetary gear, obtained with the CAD software. The gear wheels that make up the assembly have the measures described in the previous paragraph, while for the flanges has been studied a different system from the one used for the gear tests.

The flanges, in fact, are composed of a coupling with interference between a PLA element (the actual flange) obtained with FDM and an outer steel ring, as shown in Figure 42. The purpose of the metal ring is to unload most of the axial component of the forces to which the gear wheels would be subjected, as previously described. The PLA flange, on the other hand, has been shaped in such a way as to allow an interference fit with the section bar on which the whole planetary gear is mounted.

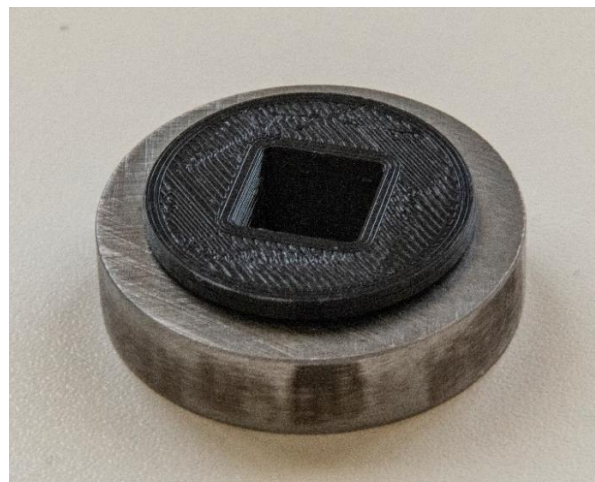


Figure 42 Assembly composed of a flange and a steel ring

The planetary gear was completely assembled by coupling the elements by interference with a hollow metal bar with square section. As already mentioned in the previous paragraph, it was necessary to redesign the coupling area between the components of the assembly and the section bar. The edge of the bar turns out to be 12 mm, consequently the seats made in the wheels have a square section with a side of 13 mm (considering the corrections which have to be made to consider the diametral error).

The square slot obtained in the gear wheels is already visible in Figure 40. A square slot with a size of 13 mm was also obtained in all the other elements coupled with the square section bar, the flanges and spacers, shown in Figure 43.



Figure 43 Flange and spacer used

A recurrent problem in the realization of the project was the difficulty encountered during assembly. Both the assembly of the planetary gears and the subsequent coupling of the planetary gears with the solar gear and the internal gears require high precision. For the coupling between the toothed gears it was necessary to take into account the exact teeth in coupling, in order not to compromise the functionality and the symmetry of the reduction gear itself.

For the final assembly of the planetary gear, the gear wheels and flanges were positioned as shown in Figure 41. Subsequently, an M8 threaded rod was inserted into the square-shaped metal section bar. The assembly was closed and locked on both sides with a self-locking nut and a castellated nut with split pin, inserted in a hole formed in the threaded rod.

The same procedure was repeated for all three planetary gears that make up the assembly, obtaining the result shown in Figure 44.



Figure 44 Final assembly of the planetary gear

Subsequently, the procedure for obtaining the solar gear is described. The solar gear can be considered as the actual junction ring of the electric motor with the designed reduction gear.

4.6. Assembly of the solar gear

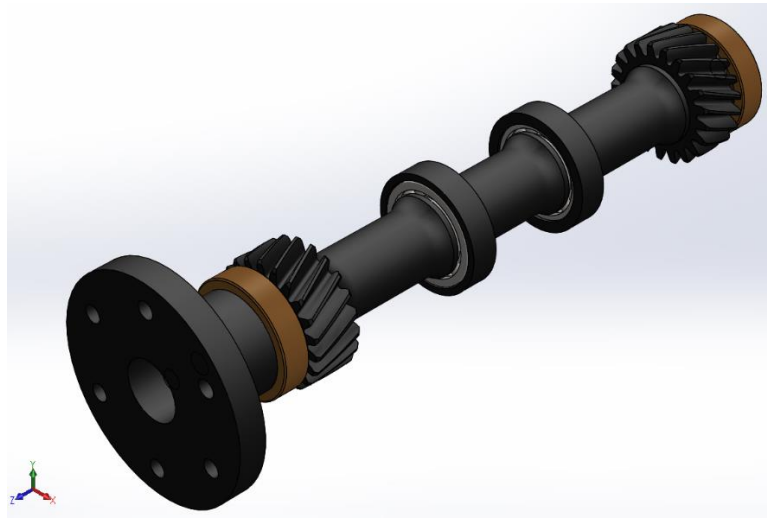


Figure 45 Drawing made with the CAD software, showing the final structure that planetary gear must have

The production of planetary gear requires the printing of three spacers, two gear wheels, two rings, four flanges and an adapter, to obtain the structure shown in Figure 45.

In addition to the listed elements, the planetary gear is composed by two steel rings, similar to those described in the previous paragraph and always with the function of unloading most of the axial load, and two steel ball bearings, with an internal diameter of 20 mm and an outer diameter of 37 mm.

The sources of criticality of this structure are two: the gear wheels and the adapter.

In a first attempt the wheels were kept the same size as those studied in paragraph 4.3. The following measurements and subsequent meshing tests with a test tothing, similar to that of the internal gear (shown in Figure 46), led to a slight modification of the project. In fact, it was necessary to reduce the width of the teeth on both wheels, to favor a better meshing, which would allow a simpler assembly, without having to force the assembly of the gears in an excessive way, risking to break the assembly itself.



Figure 46 Test tothing that reproduces the internal gear

The main function of the adapter is to connect the reduction gear with the flange of the electric motor, in order to activate the rotation of the system. However, while to obtain the holes for the coupling with the steel flange of the motor no particular attention was required during the preparation phase for the printing, the production of the lower hole required the addition of the support structures.

Before choosing this solution, different design alternatives were considered, but none allowed to obtain the space necessary to accommodate the nut screwed onto the threaded rod (M8, of the same type as those mounted on the satellites), without the latter leaking out from the adapter structure; it is necessary that the threaded rod and the nut are contained in the adapter slot, to avoid interference with the flange with which the adapter must be coupled. The area to which reference is made is shown in the sectional view in Figure 47.

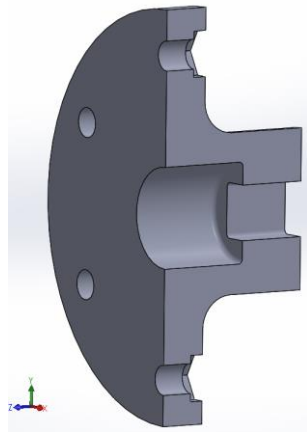


Figure 47 Section view of the adapter, to highlight the area that houses the nut

The supports used to manufacture the lower bore of the adapter are of the "zig zag" type, as indicated on the Ultimaker Cura software. The characteristic of these supports is the simplicity of removal, although they are produced of the same material as the piece. The finishing obtained once the support structures have been removed is poor, negligible problem, since no particular precision is required in the contact between the nut and the lower surface inside the hole.

The final design of the adapter is shown in Figure 48.

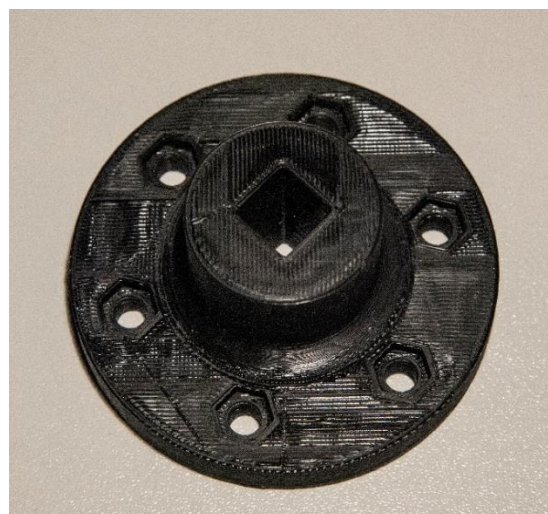


Figure 48 Final design of the adapter

Furthermore, it was necessary to print the PLA rings to be coupled with the bearings used (as shown in Figure 49). These rings must remain in contact with the metal rings on the sides of the double-helical gear wheels, and therefore require a slightly more accurate surface finish than the other parts produced.



Figure 49 Coupling of a bearing with the PLA outer ring

Once all the elements of the assembly were individually studied and printed, it was possible to obtain the final structure of the solar, shown in the figure.

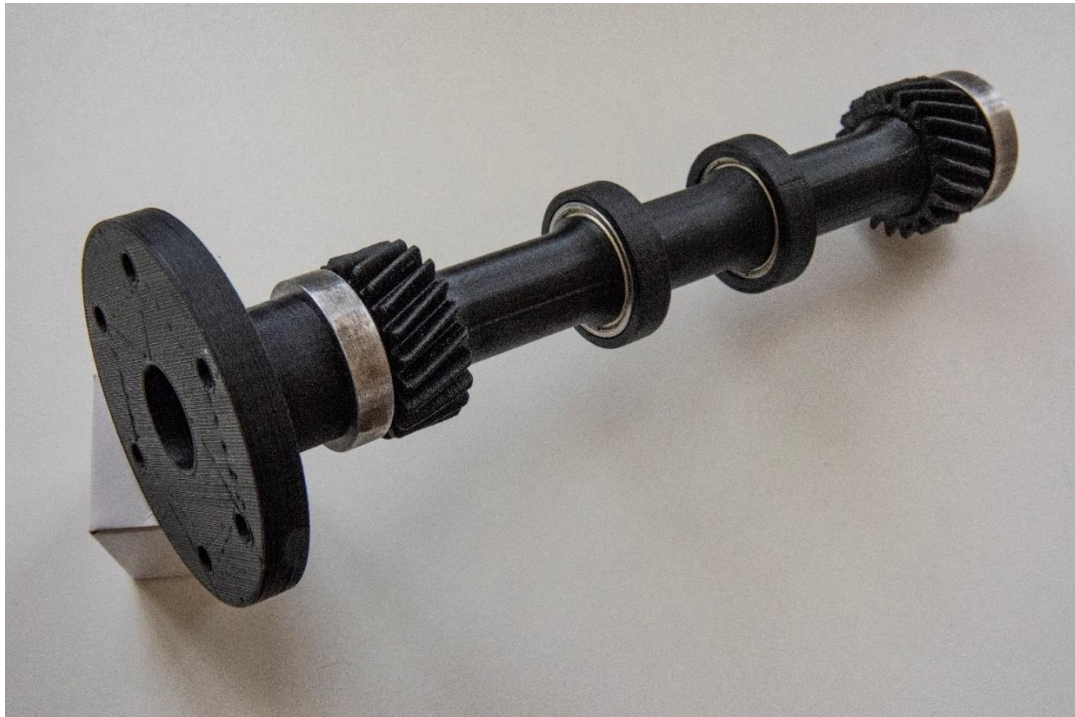


Figure 50 Final assembly of the rotating solar A

Therefore, the design and printing work can proceed with the structural study and production of the internal gears of the reduction gear and with the meshing tests of the components obtained up to now.

4.7. Design of the internal gears

The next step was to redesign and print the internal gears, following the constraints imposed by the single nozzle FDM technique and taking up what was already done in the design stage of the gear wheels.

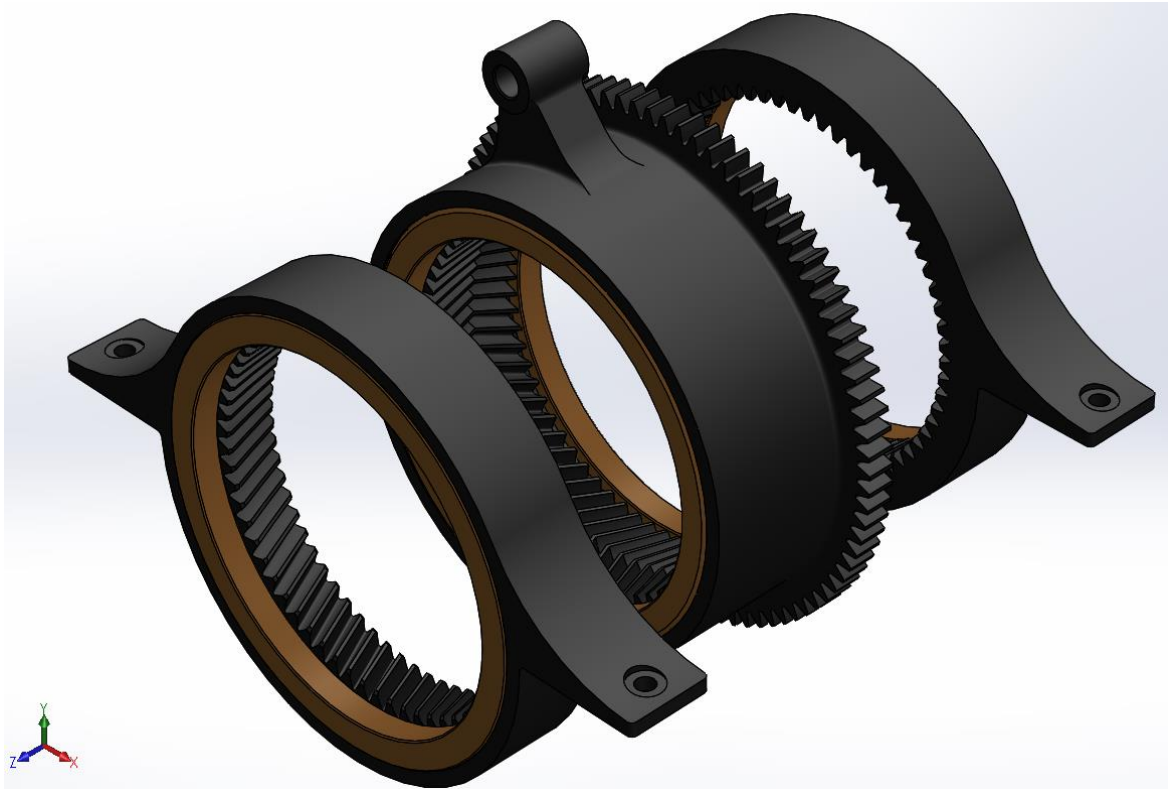


Figure 51 CAD design of the internal gears of the reduction gear

Observing Figure 51, it can be seen that the two side crowns are almost identical, except for the angle of inclination of the teeth, while the central crown (with a double-helical structure) has a very different structure from the other two.

For this reason, it was necessary to analyze the components in two separate steps, so as to obtain the correct meshing and the appropriate measures first, then a simple structure to be printed, which should not require the use of the support structures.

4.7.1. Design of the lateral internal gears

In order to be able to switch to the production of the lateral crowns (Figure 52), it was first necessary to perform print tests. The parts taken into consideration, in fact, are much larger than all the other components produced previously, so the first datum to be obtained was the one concerning the influence of thermal shrinkage in the printing phase.

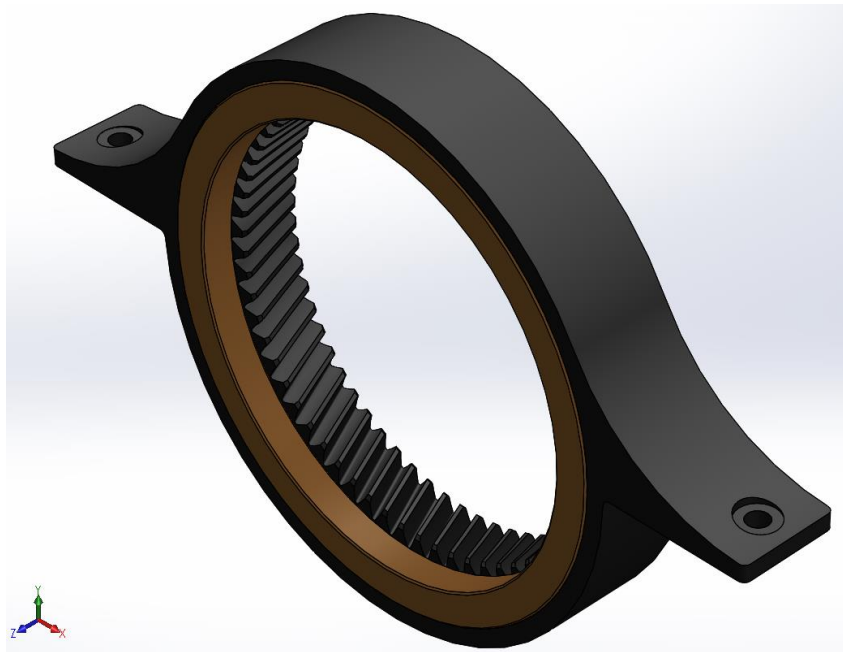


Figure 52 CAD design of one of the two lateral internal gears

Following a first print (the result of which is shown in Figure 53), measurements were taken with a caliber, to compare the result with the reference CAD. In this phase it was necessary to obtain the measurement of the internal coupling diameter with the steel ring (colored brown in Figure 52).

The nominal value of this diameter is 146 mm, while, on the basis of the obtained measurements, the external diameter at the end of printing is 144 mm. Therefore, the error due to thermal shrinkage for pieces of dimensions that tend to the maximum size of the printing table (177.8 x 177.8 mm) is about 2 mm.



Figure 53 First printing result of the lateral internal gear

In the second printing attempt, following the result obtained with the analysis of the thermal shrinkage, the design was corrected to the CAD software, resizing the internal diameter for the coupling with the steel ring. Moreover, thanks to the considerations on the gear made in third paragraph in this chapter, the profile of the crown teeth was corrected, reducing the thickness from the result shown in Figure 54 to that shown in Figure 55 (the thickness value was halved).



Figure 54 Detail of the teeth profile obtained with the first attempt



Figure 55 Profile of the teeth obtained in the second attempt, following the narrowing of the profile

Having performed the corrections described above, it was possible to obtain the complete structure of the first side crown, shown in Figure 56.



Figure 56 Final structure of the side crown, coupled with the steel ring

To obtain the second external crown, it was sufficient to mirror the structure obtained with the CAD software, thus maintaining the structure unchanged.

It should be noted that the printed structures are very large, so one of the main objectives was to reduce the number of printing tests to a minimum. An internal gear of the dimensions shown in this paragraph, in fact, requires a printing time of 13 hours and 46 minutes, considering the speed of the of 30 mm/s.

This particular attention to the printing times and to the expense of material required for the production of large components will guide the design of the central internal gear, the largest component in the whole assembly.

4.7.2. Design of the central internal gear

The final step in completing the construction of the conceptual prototype of the reduction gear is the production of the central internal gear. This component has a double-helical internal gear, for coupling with the central wheels of the planetary gear, and an external spur tooting, for coupling with the straight-toothed wheel of the encoder of the test bench.

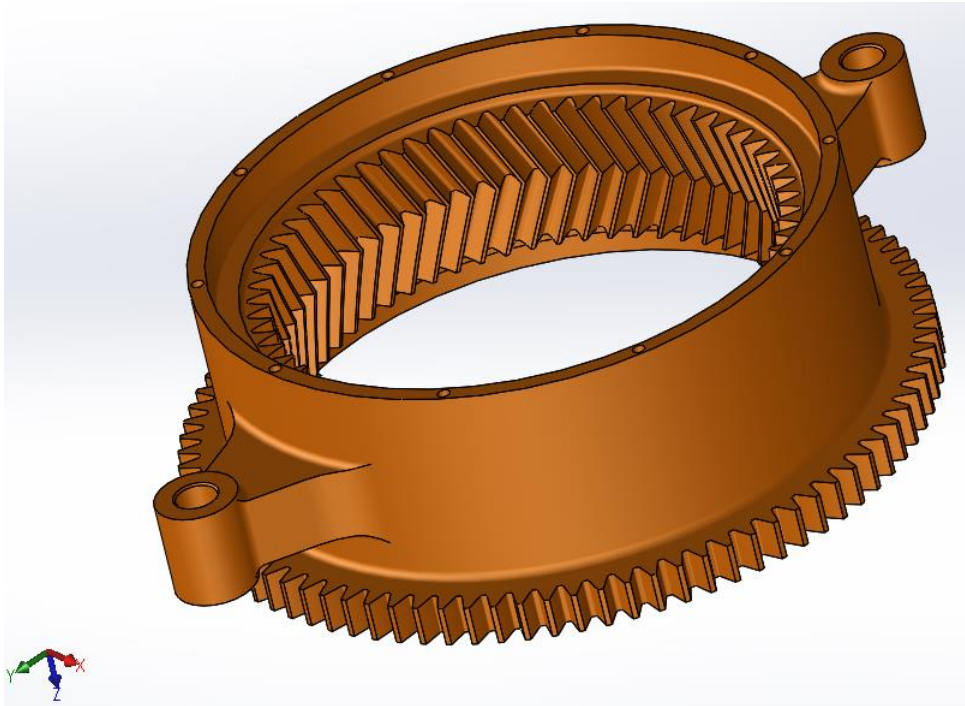


Figure 57 Central internal gear of the reduction gear

The component has been reported in Figure 57 with a different color from the final one (which will be black), in order to better highlight the constructive criticalities. After a careful analysis of the piece, it can be seen that the side elements are, in fact, the most critical components for the production of the piece for FDM. These two elements would require the generation of support structures that should be in contact both with the printing plane and with the external teeth. While the contact of the support structures with the printing plate does not create any problem, if not a lengthening of the production times, the construction of supports that touch the external tooting risks to affect the surface finish of the component in this area, compromising the functionality and generating an irregularity on the profile of the tooting itself.

The first possibility studied was to turn the piece upside down on the printing surface, keeping the tothing upwards and avoiding the generation of supports inside the external tothing. This idea was immediately discarded, as the production of the piece would have required a production time of about two days. The cause of the particularly long times is due to the generation of a very relevant support structure. Another criticality derives from the fact that, even in this case, the Ultimaker Cura software recommends creating the supports between the teeth and the side elements. It would therefore risk to ruin the piece and compromise its functionality in the attempt to remove the support structures from the piece oriented in the position just described.

The next option taken into consideration, therefore, was that of the redesign of the component, in order to be able to produce it more simply for FDM.

First of all, a subdivision of the component has been studied to avoid the generation of support structures inside the spur outside gear. For this reason, the piece has been decomposed, disconnecting the side elements to be able to produce them separately. For the subsequent positioning of these elements in the final component, two slots have been designed for coupling in the central crown, as shown in Figure 58.

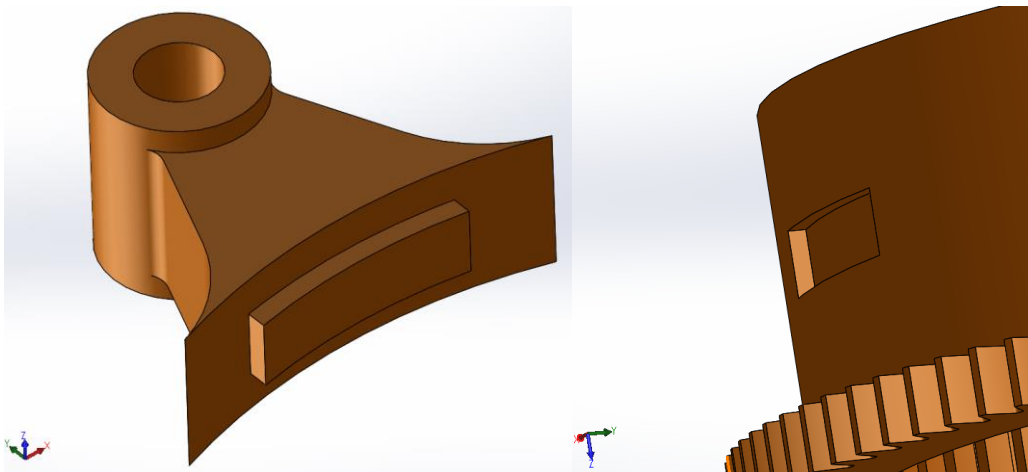


Figure 58 Detail of one of the two side elements with the corresponding slot, after the redesign

The elements described above are not subjected to high loads during operation; for this reason, the designed fixing and a subsequent gluing and pressing are sufficient to keep the side components in position.

The final result of this coupling, once assembled, is shown in Figure 59.



Figure 59 Final result of the coupling between the outer component and the side elements

Another critical element is the double internal fillet, visible in Figure 57, designed as a slot for the steel ring in contact with the wheel rings of the planetary gears. Also in this case it would be necessary the generation of support structures which would be too complicated to remove, always bearing in mind that for FDM single nozzle there is no possibility to produce soluble supports. To solve this problem, a subdivision between the outer element with spur gear and the internal toothed area has been studied. The two parts were separated at the coupling area with the steel ring. To allow the subsequent coupling between the pieces, a system of 60 radial "teeth" has been studied, with a thickness and a width of 2 mm.

This system, of which the two components have been reported in Figure 60, makes it possible to have a simple and robust coupling between the internal double-helical toothing and the part which includes the external spur toothing, making the use of gluing unnecessary, since the toothing will be locked in the correct position by the steel rings.



Figure 60 Detail of the coupling between the outer part and the inner part with the double-helical toothing

As for the outer crowns produced previously, a correction of the internal toothing was necessary, halving the thickness of the teeth themselves, to favor a better meshing between the internal gear and the double-helical gear wheels.

Moreover, due to the high dimensions of the component (similar to those of the lateral internal gears described in the previous paragraph), an increase in the size of the internal and external diameters of 2 mm was necessary to compensate for the thermal shrinkage caused by the production technique and by the use of PLA, as already described in the previous chapters.

Figure 61 shows the exploded view of the final assembly that makes up the central internal gear.

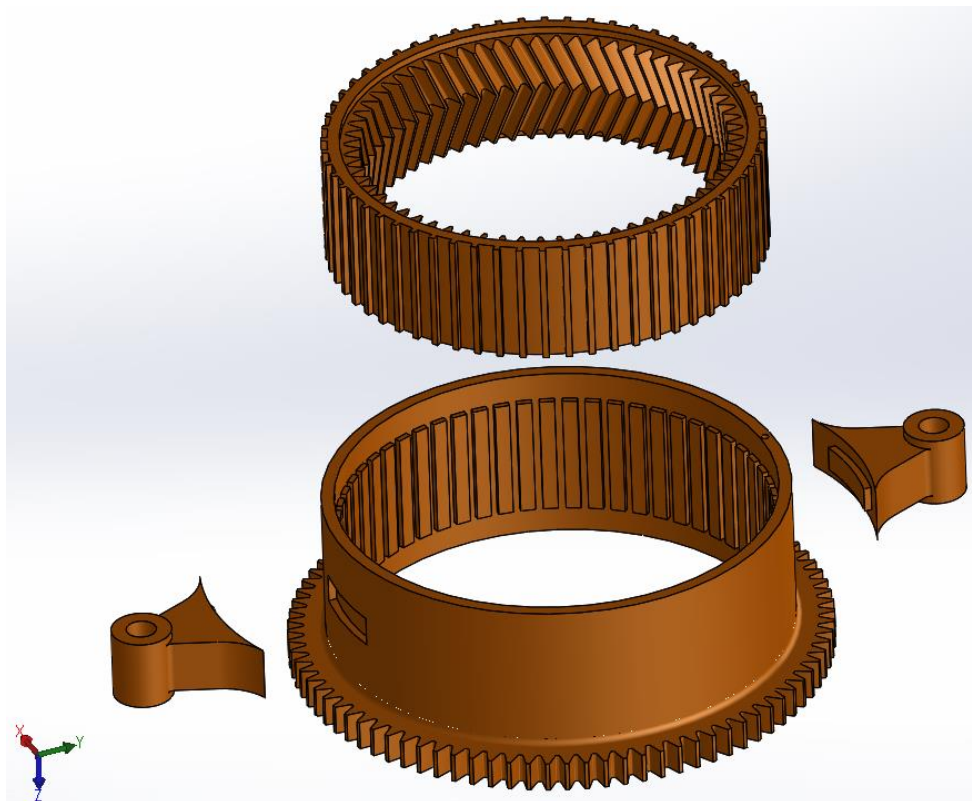


Figure 61 Exploded view of the central internal gear, after redesign operations

4.8. Assembly of the reduction gear

As already mentioned, the most critical phase for the realization of the reduction gear consists in the final assembly. This phase is complex, as it requires the participation of at least two people in order to be completed.

The gear wheels at the ends of the satellites are composed of twenty-one teeth and must be meshed with the respective outer crown, whose toothing is made up of sixty-three teeth. It is particularly important to take this problem into account, as it was necessary to perform a calculation of the teeth themselves, before meshing the gear wheels with the lateral internal gear.

Furthermore, to facilitate the assembly phase, it was necessary to separate the individual pieces that make up the planetary gears and the rotating solar A. This arrangement allowed us to carry out the teeth account described above and made it possible to assemble the segments from which the reducer is formed in successive steps, without requiring, therefore, the subdivision of the lateral internal gears into two shells each. Cutting the lateral internal gears into two distinct elements could have caused more imperfections, leading to misalignment in the assembly of the finished component.

The first step was, therefore, the meshing of the end wheels with the lateral internal gears. This first coupling was constrained with the addition of the metal ring inside the groove in the lateral internal gear and with the insertion of the external metal rings on the flanges, coupled together with a very small clearance (about 0.1 mm).

Subsequently, it was possible to insert the square section hollow metal profiles in the special slots formed in the gear wheels. Once the spacers were added, the next step was the insertion of the double-helical gear wheels, flanked by their respective flanges and metal rings, then coupled with the two bearings mounted on the central shaft of the rotating solar A.

The subdivision of the central internal gear into several components allowed the use of the part with the internal teeth for the first coupling with the double toothing wheels, instead of preassembling the entire structure created. The section with internal teeth alone is less bulky and, therefore, easier to handle during assembly. Once the gear wheels have been positioned at the correct angle, the central internal gear has been closed, coupling the internal toothing area with the outer shell and closing the assembly with the two steel rings.

During the design phase, on the gear wheels at the ends of the planetary gears, a slight blind hole has been created; it allows to have a reference during assembly, so as to be able to position the gear wheels at the opposite ends of the reducer correctly in terms of orientation on the square-based metal profile. This hole also makes teeth counting easier. Bearing in mind what has just been said, the gear wheels at the free end have been inserted on special supports with a square base.

Later, the missing lateral internal gear was inserted, following the tooth counting procedure described at the beginning of this paragraph. This step is simpler than the one described initially, since, if the procedure has been followed correctly, the gear wheels of the second end will not require repositioning and the lateral internal gear can be easily inserted, following the angle of the teeth.

The slight interference (already mentioned and described in the previous paragraphs) between the metal profiles and the elements obtained from the print and coupled with the profiles themselves, made it possible to simplify the assembly and arrangement operations of the assembled pieces.

Once the reduction gear component positioning procedure was completed, the steel rings inserted in the internal gears were fixed to the slots through the use of washers, locked with self-threading screws. The use of this coupling required particular attention in the preparation phase for the printing. The design of the lateral internal gears, in fact, has been modified, with the addition of ten blind holes with a diameter of 3 mm, having the function of guiding the self-threading screws. In addition, to prevent the insertion of the screws compromising the structural integrity of the lateral internal gears, a thickness of two layers was added around the “invitation” holes, so as to offer the screws a greater quantity of material for the threading.

The reduction gear obtained at the end of the assembly phase is shown in Figure 62.

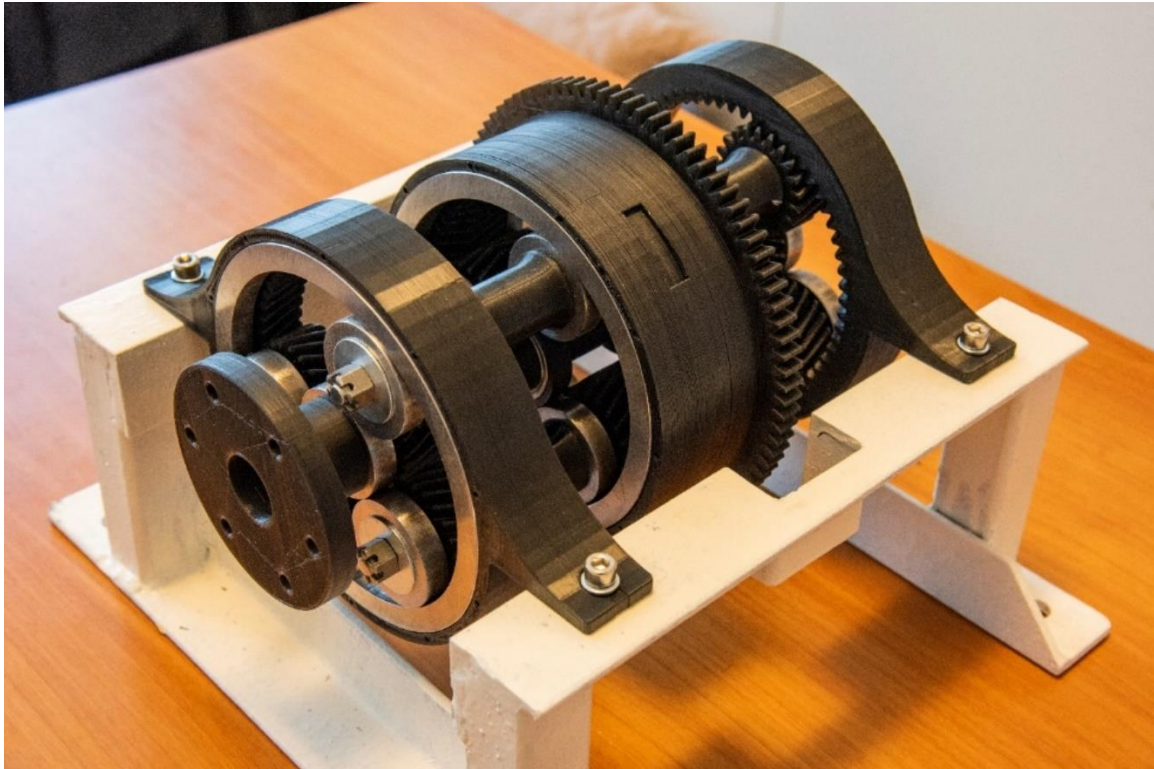


Figure 62 Reduction gear assembled

Once assembled, it was possible to glue the side coupling pieces of the central internal gear with the encoder, which will be inserted next to the reducer structure itself.

4.9. Coupling between the reduction gear and the encoder

As already mentioned, the reduction gear produced during this thesis will be used for educational purposes in the laboratories of DIMEAS (Department of Mechanical and Aerospace Engineering), in order to reproduce the operation of a reduction gear within a real EMA.

In order to be able to perform measurements on the reduction gear, two main systems have been devised: a strain gauge system, which detects bending stresses on the external crowns of the mechanism, and an encoder, connected to the central crown of the reducer itself.

The coupling between the reduction gear and the encoder has been realized by connecting a spur gear wheel to the encoder, coupled to a support by means of two roller bearings (of the same type and of the same size as those used on the rotating solar A). The spur gear wheel meshes with the external teeth of the central structure of the reduction gear (or rotating solar B) and the wheel shaft has been connected to the encoder itself with an interference fit. In this way, the encoder records the rotation of the gear wheel, allowing to calculate the movement of the rotating solar B.

Figure 63 shows the support used and the spur gear wheel coupled with the encoder.

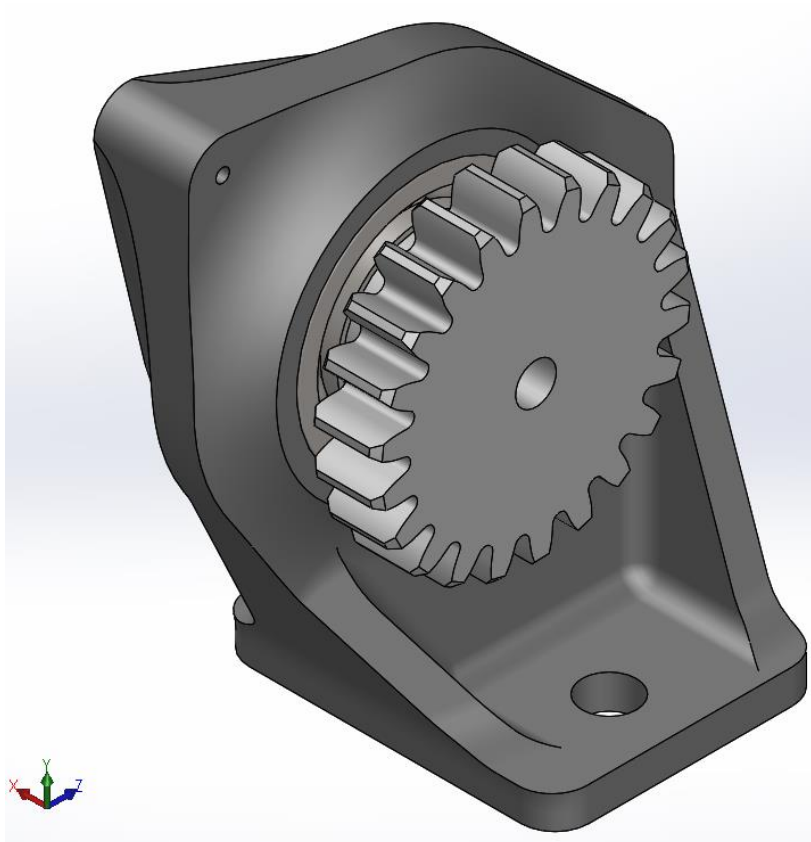


Figure 63 CAD drawing of the coupling between the support for the encoder and the spur gear wheel

4.9.1. Encoder utilized

The encoder used for this project is TSW581HS.M2.5000.5.V.K4.B127.PL10.PP2-5. The code given contains the characteristics of the type of encoder used, in the range of products provided by the Italsensor company for models TSW58HS. The characteristics, therefore, are shown in

Model	TSW581HS	Bidirectional with index
Assembly type	M2	With spring type M2
Pulse rate	5000	
Power supply	5	+5 V
Output frequency	V	From 0 a – up to 300 kHz
Protection degree	K4	IP 64 (EN60529)
Shaft diameter	B127	12,7 mm
Electrical connections	PL10	Cable length of 1 m
Output Circuits	PP2-5	Push-Pull 5 V output only

Table 3.

Model	TSW581HS	Bidirectional with index
Assembly type	M2	With spring type M2
Pulse rate	5000	
Power supply	5	+5 V
Output frequency	V	From 0 a – up to 300 kHz
Protection degree	K4	IP 64 (EN60529)
Shaft diameter	B127	12,7 mm
Electrical connections	PL10	Cable length of 1 m
Output Circuits	PP2-5	Push-Pull 5 V output only

Table 3 Characteristics of the encoder used for rotation detection

This tool carries out the measurement of the degree of rotation of the rotating solar B, following an input sent to the rotating solar A by the electric motor.

The data detected by the encoder can be saved and analyzed later. The high number of pulses per revolution (5000), combined with the fact that it is a bidirectional encoder, allows high precision in detecting displacements.

It is possible, by measuring the rotation of the gear wheel connected to the encoder itself, to obtain the real position of the rotating solar B. Later, we can go back to the ideal position of the rotating solar B, thanks to the data calculated on the reduction ratio. The comparison between these two detected positions allows to obtain the positioning error caused by the inaccuracies of the reducer structure produced with FDM.

4.9.2. Support for the encoder

The support for the encoder (whose CAD drawing is shown in Figure 64) required, in the design phase, particular attention to some aspects.

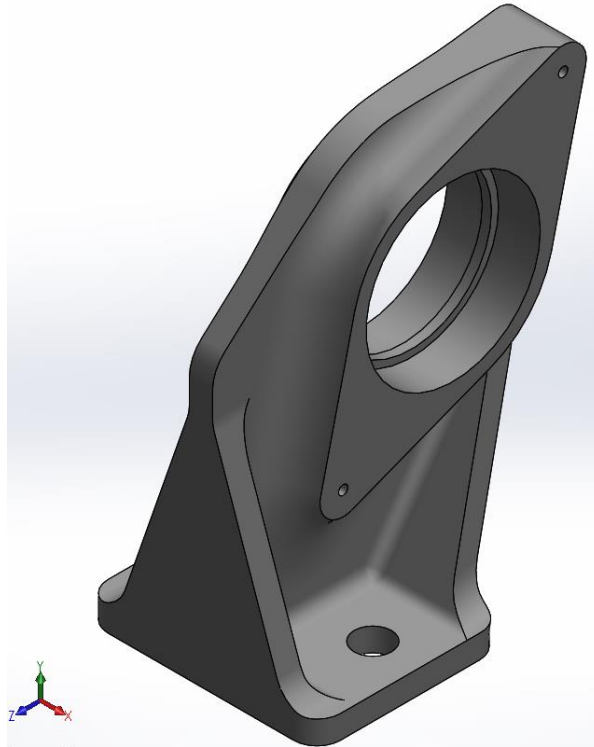


Figure 64 CAD drawing of the encoder support

First of all, this component must be able to be coupled with a slight interference with the two bearings that allow the connection with the gear wheel shaft. For this reason, the cylindrical coupling section with the bearing slot was produced with an internal radius of 38 mm, in order to obtain a final diameter of 37 mm (due to the effects of thermal shrinkage, seen in the previous paragraphs).

With the first print, a first problem was highlighted: the complexity of the piece and, therefore, the continuous changes of direction to which the nozzle must be subjected require a modification of the production parameters. The problem emerged following a failure of the first production attempt. The nozzle stopped dispensing the necessary filament, which allowed to understand how the solution could be a reduction in the speed of displacement of the nozzle during printing. The displacement speed, therefore, has been reduced from 30 mm/s to 25 mm/s.

Moreover, in order to have a better finishing of the piece, the thickness of the layers was brought from the value of the "Normal" setting (0.15 mm) to the value of the "Fine" setting, which means 0.1 mm.

Both the solutions used to improve the finishing and production of the piece have led to a net increase in production times (from 4 hours and 21 minutes, initially planned, to 6 hours and 31 minutes, used to complete the second attempt).

In addition to the problems related to print data, it was necessary to redesign the component to avoid contact with the external spur gear of the reduction gear. The lateral rib of the support, in fact, interfered with the rotation of the central crown, risking breaking one of the two components. The redesign, consisting in a removal of material, made it possible to shorten the printing times slightly.

The second printing attempt revealed two fundamental problems:

- a) The transition to the "Fine" setting causes a reduction in the effect of thermal shrinkage; for this reason, the diameter of the coupling with the bearings has been increased to the value of 37.5 mm on the CAD file (the error, therefore, is halved).
- b) The significant dimensions of the coupling hole make its production being impossible without the addition of internal support structures. In the next attempt, therefore, the internal support structures were added to the hole, whose production caused an increase in printing time of 2 hours, bringing the total time to 8 hours and 31 minutes.

The result of the third and last printing attempt is reported in Figure 65.



Figure 65 Support for the encoder

4.9.3. Spur gear wheel

Once the support production was completed, the design continued with the analysis of the coupling component between the rotating solar B and the encoder. This coupling has been realized with a spur gear wheel, which meshes with the teeth of the central component of the reduction gear, and with a shaft of variable section, obtained in the center of the same gearwheel. The solution for the coupling just described is shown in Figure 66.

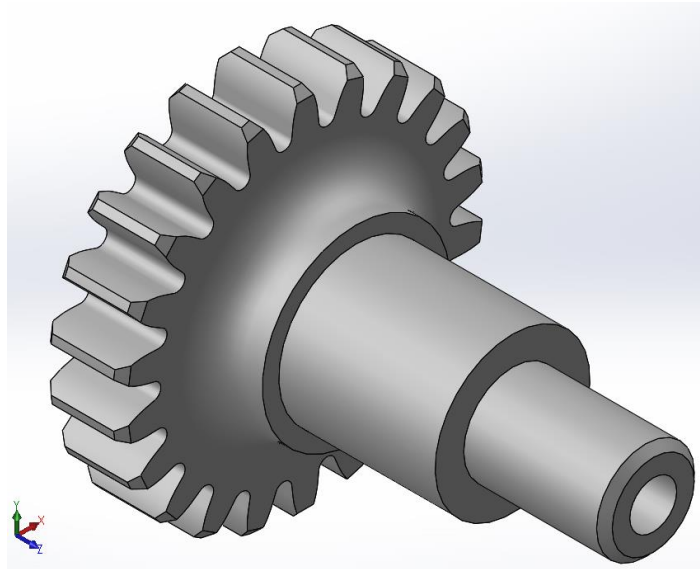


Figure 66 CAD drawing of the coupling wheel between the encoder and the rotating solar B

A first printing attempt was made to analyze the criticality of the component, using the same settings used to produce the support for the encoder. As for the printing of the support, even the first attempt to produce the shaft with the gear wheel was unsuccessful and made it possible to detect the two main sources of error:

- a) The machine must accommodate three sudden section changes. This problem was solved by inserting a fillet with a radius of 5 mm between the gear wheel and the shaft, to make the section change more gradually, and reducing the deposition speed from 25 mm/s to 20 mm/s, to allow the nozzle to supply the necessary material once positioned on the new deposition area.
- b) The cylindrical section of the shaft having a diameter of 12.5 mm is liable to incur delamination, which means that there is a risk that in this section there may be a separation of two consecutive layers, if the piece is stressed with a shear stress. The reduction in the deposition speed also affects this problem, but, to further increase the strength of this section, the thickness of the walls was increased (from 0.8 mm to 1.6 mm) and a central through hole of 5.5 mm was made; this hole allowed to insert a metal rod in the component.

The second and last printing attempt, with the changes made, required about twice the printing time compared to the time taken to produce the first attempt.

The component obtained at the end of printing is shown in Figure 67.

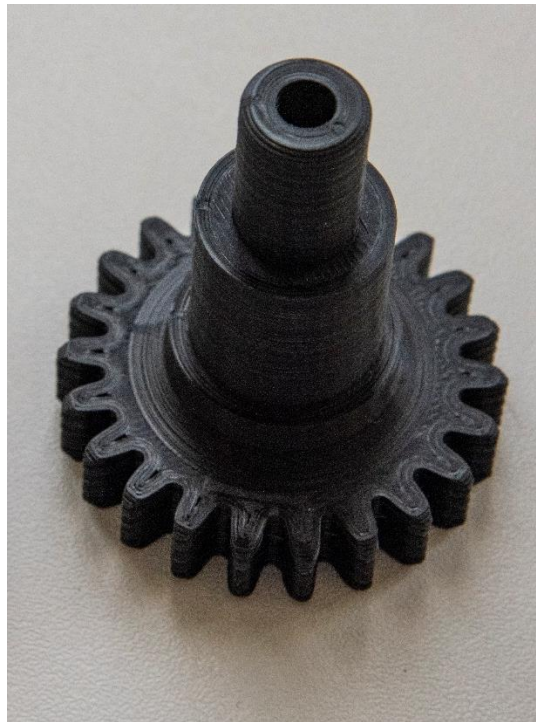


Figure 67 Coupling gear wheel between the encoder and the rotating solar B

5. Future developments and conclusions

Once the analysis of the design and construction of the reduction gear has been completed, it may be interesting to define what future developments of the project might be, in terms of resizing the components and structural improvement, and what the end use of the reduction gear itself will be.

5.1. Future developments

First of all, the practice of constructing the reduction gear has made it possible to detect the main problem in the production of the component: the assembly.

The assembly of the reduction gear, as already anticipated, requires the presence of at least two people, since some positioning of the components requires the use of four hands. Two notable examples are the placement of the gear wheels that mesh inside the lateral internal gears and the forcing of the flanges at the end of the assembly. The latter requires a preload on the flanges already positioned, while a second operator takes care of inserting the last flange in the assembly.

In the design phase, some references were provided to facilitate final assembly, references that required, however, to make a teeth count, to define the meshing. In the event of a redesign, it may be useful to study more suitable references, so as to make the account of the teeth superfluous.

To simplify the assembly, it would be appropriate to revisit the architecture of the reduction gear, in order to make it more compact; in fact, the structure of the reduction gear produced is "exploded" for purely didactic reasons, since the presence of the spacers allows to observe the internal functioning of the components.

Another method to facilitate the assembly could be the execution of a redesign more oriented to the final assembly.

The assembly of the current reducer, in addition to the presence of two people, also requires the decomposition of the satellites and of the rotating solar A, in order to start from the meshing of the gear wheels with the side internal gears and continue with the assembly of the satellites and the rotating solar A on the gear wheels positioned. This method requires the teeth to be counted for each of the two lateral internal gears. While the counting and the meshing of the gear wheels of the first lateral internal gear is simpler, the insertion of the final gear wheels involves some difficulties.

Redesigning in an "assembly-oriented" manner, would mean recalculating the number of teeth of the reduction gear components, so as to obtain a multiple of 3 as the number of teeth inside the central component. This would allow the teeth count to be performed only on the rotating solar B, allowing the satellites to be kept completely assembled during assembly and only the rotating solar A to be assembled piece by piece. Furthermore, it is important that the number of teeth on the lateral crowns is also a multiple of 3, to avoid excessive interference when inserting the outer crowns themselves.

From the formulas of paragraph 4.2. the following numbers of teeth can be obtained, starting, for example, from $z_1 = 18$, $z_2 = 36$ and $z_3 = 33$:

$$\begin{cases} z_4 = z_1 + 2z_2 = 90 \\ z_5 = z_1 + z_2 + z_3 = 87 \end{cases} \Rightarrow \tau = \frac{1 + \frac{z_1}{z_4}}{\frac{z_1}{z_4} - \frac{z_1 z_3}{z_2 z_5}} = 116$$

The numbers of teeth on the wheels of the planetary gears and in the internal gears increase, consequently the radii of these wheels increase. In the event of a redesign, this factor should be taken into account, since the risk would be that of not having sufficient space on the deposition plan for the production of external crowns. Possibly, a reduction of the toothed wheel modulus (currently 2 mm, unchanged compared to the original design) would reduce the radius of the gear wheels themselves, allowing to cover solutions with a greater number of teeth. The cost of modifying the modulus would be that of having to repeat all the meshing tests, in order to be able to carry out the necessary corrections for the manufacturing through FDM. With a reduction of the modulus to 1.5 mm, the primitive radii of the wheels would be slightly greater than those of the initial project, as shown in Table 4:

r_1	13.5 mm
r_2	27 mm
r_3	24.75 mm
r_4	67.5 mm
r_5	65.25 mm

Table 4 Example of variation of gear wheel radii in the event of changes to the modulus and the number of teeth

The reduction ratio decreases slightly, thanks to the reduction in the number of teeth of the gear wheels forming the rotating solar A (z_1) which, therefore, will have a smaller size than that of the original project. For the example given, an entire reduction ratio was sought, with the aim of facilitating the calculations during the measurement with the encoder (as already happened for the creation of the original project).

It would be possible to increase the reduction ratio by increasing the number of teeth of the gear wheels that make up the satellites, always trying to obtain a number of teeth on the internal wheels that is multiple of 3, to facilitate assembly.

For the example given, the numbers of teeth of the internal gears are multiples of 3, so the assembly could be done in four simple steps:

- 1) Teeth account and search for the mesh between the central internal gear and the herring-bone gears, locked in position by the two metal rings.
- 2) Insertion of the side gears of the rotating solar A, performing the meshing with the side gears of the satellites.
- 3) Insertion of the two lateral internal gears, held in place by the metal rings.
- 4) Insertion of the outer flanges of the satellites and of the rotating solar A and addition of the adapter.

In addition to the difficulty encountered in assembly, another limit to the production of the reduction gear was imposed by the machinery used to manufacture the parts. The fact of having a single nozzle FDM machine did not allow the production of support structures that were easy to remove, making it necessary to redesign some components that, with a multiple nozzle printer, could have been produced as designed in the first project.

The limits due to the material used are also related to the machinery. To have superior mechanical characteristics, it would have been useful to produce the ABS components, using, where necessary, PVA support structures. It was not possible to use the materials mentioned, as the machine used is open chamber, so it would not allow to dispose of the toxic fumes produced by the melting of the ABS. Furthermore, since it is not possible to produce soluble support structures, the orientation alternatives of the pieces produced on the deposition plane were particularly reduced.

Another limitation of the machine used is the reduced size of the printing plan. With the dimensions of the printing surface of a machine like the Fortus 250mc (254 x 254 mm), produced by Stratasys, a reduction gear could be created with the specifications described on the previous page, without the need to make changes on the toothed wheel module; or a larger reduction gear could be produced, reaching a reduction ratio of 175.

A machine that fits the characteristics described, however, would require a considerable investment of money.

5.2. Conclusions

At the end of the assembly of the reduction gear, it was possible to verify how the poor surface finish and the high tolerances, weak points of the additive manufacturing compared to the traditional manufacturing, caused an axial displacement of the satellites with respect to the lateral internal gears, secured to the base. This phenomenon occurred by rotating the gear by hand, therefore with loads much lower than those that the reducer would have had to withstand during use, and was due to internal mechanical frictions caused by poor surface finishing.

To correct the defect just described, two washers were added at the ends of each satellite; those washers have a diameter of 48 mm, which is, therefore, greater than that of the metal rings coupled with the flanges. In this way, the structure is stable and a resistance to the axial displacement of the satellites is introduced.

Once the gears have been lubricated, the rotation tests without load can be performed by simply connecting the reducer to the electric motor. If the reduction gear will also pass these tests, it can be used for the didactic purpose set and described in the introduction.

The reduction gear will be part of the test bench of an EMA, on which two different types of load tests can be performed:

- a) A load test on the engine.
- b) A load test on the reduction gear itself, made by connecting a spring on one of the two lateral ends, mounted on the outside of the central crown.

Taking advantage of the potential of additive manufacturing, an integration of sensors could be evaluated, located directly in the structure of the reduction gear. In particular, it would be useful to consider the integration of innovative sensors, characterized by limited encumbrance, placed in such a way as to detect information for the control and monitoring of the system.

Bibliography

- [1] **L. Iuliano.** *Tecniche di fabbricazione additiva – Dispense del corso.* Politecnico di Torino (2018).
- [2] **P. Fino.** *Materiali per la fabbricazione additiva – Dispense del corso.* Politecnico di Torino (2018).
- [3] **M. D. L. Dalla Vedova.** *Tesi di dottorato – Comandi di volo ed introduzione al problema dell'asimmetria.* Politecnico di Torino.
- [4] **G. Riva.** *Tesi di laurea triennale – Studio di modelli numerici a parametri concentrati per la modellazione di servovalvole.* Politecnico di Torino (2016).
- [5] **P. Maggiore.** *Sistemi di bordo aerospaziali – Dispense del corso.* Politecnico di Torino (2013).
- [6] **P. Maggiore.** *Modellazione, simulazione e sperimentazione dei sistemi aerospaziali – Dispense del corso.* Politecnico di Torino (2015).
- [7] **A. Gugliotta.** *Costruzione di macchine – Dispense del corso.* Politecnico di Torino (2017).
- [8] **Ultimaker.** *Ultimaker Cura Software Manual.* Online: <https://ultimaker.com>
- [9] **Dddrop.** *What are the advantages of the FDM technology.* Online: <https://www.dddrop.com/fdm-technology/>
- [10] **Stratasys.** *Materials data.* Online: <https://www.stratasys.com/it/materials>